Infrared Physics & Technology 137 (2024) 105114



Contents lists available at ScienceDirect

Infrared Physics and Technology

journal homepage: www.elsevier.com/locate/infrared



Recent progress of innovative infrared avalanche photodetectors

Shuning Liu [a], Qi Han [b], Wenjin Luo [c], Wen Lei [d], Jun Zhao [e,*], Jun Wang [b,**], Yadong Jiang [b], Markus B. Raschke [c,***]

[a] Hangzhou Institute for Advanced Study, University of Chinese Academy of Sciences, Hangzhou 310024, China
[b] School of Optoelectronic Science and Engineering, University of Electronic Science and Technology of China, Chengdu 610054, China
[c] Department of Physics and JILA, University of Colorado, Boulder, CO 80309, United States
[d] Department of Electrical, Electronic, and Computer Engineering, The University of Western Australia, Perth, WA 6009, Australia
[e] Kunming Institute of Physics, Kunming 650223, China

A B S T R A C T

Currently, the development trend of infrared detection systems is oriented towards achieving smaller size, reduced weight, lower power consumption, decreased cost, and heightened performance, collectively referred to as SWAP^3. In this context, a rapid evolution is witnessed in the realm of next-generation high-sensitivity infrared avalanche photodiodes (APD). In recent years, the increasing demands for detector performance from astronomical, remote sensing, and civilian applications have presented novel challenges for the mechanistic exploration and device design of traditional avalanche photodetectors. This review explores the forefront of infrared APD technology, focusing on the remarkable progress achieved through the utilization of II-VI and III-V semiconductor families and the exploration based on novel low-dimensional materials. The review provides a detailed analysis of the unique properties and performance enhancements exhibited by APDs based on these material systems, shedding light on their potential for revolutionizing infrared sensing and imaging applications, and inspiring further innovation and exploration in the field of infrared photodetection.

1. Introduction

As an electromagnetic wave, infrared radiation can interact with vibration modes or with electrons in infrared detection materials. These two interactions correspond to two types of infrared detectors: thermal detectors and photon detectors. Compared to thermal detectors, infrared detectors based on the photoelectric effect have high signal-to-noise ratio (SNR) performance and very fast response. Therefore, infrared photoelectric detectors are more inclined to be used in infrared detection systems requiring higher reliability and sensitivity. In 1959, Lawson and his colleagues in the UK synthesized HgCdTe, which exhibited excellent infrared detection performance and played an important role in the development of entire infrared detection technology. In addition, with the gradual development of silicon technology, non-intrinsic Si materials have also attracted considerable research interest and quickly moved toward practical applications. After entering the 1980 s, with the development of material growth processes (molecular beam epitaxy, metalorganic vapor phase epitaxy), material growth could be precisely controlled. A series of materials based on band engineering, such as superlattices, quantum wells, and some new materials at that time, such as InGaAs, were successively developed, further expanding the selection of infrared detection materials[1,2]. In the 21st century, advancements in material growth processes have facilitated the emergence of novel structures built upon superlattices and quantum wells, such as quantum cascade detectors and interband cascade detectors. In recent years, low-dimensional materials-based infrared detectors, represented by graphene and black phosphorus, have demonstrated excellent infrared detection capabilities at room temperature, with the potential for further applications. Infrared detectors with photon number resolution capability are an important research focus of the new generation of infrared detection systems[3–5]. For infrared light, the energy carried by an individual photon is less than that of visible light. For example, in the 5 μm wavelength band, the energy of a single photon is approximately 3.98×10^{-20} J, which is nearly an order of magnitude lower than that of visible light. Achieving detectors capable of resolving such extremely low-energy and photon numbers presents a significant challenge.

Avalanche photodiodes (APD) represent a feasible method for detecting extremely weak infrared light signals. For extremely weak light signals, or light-induced signals without internal gain, signal

* Corresponding author at: Kunming Institute of Physics, Kunming 650223, China.
** Corresponding author at: School of Optoelectronic Science and Engineering, University of Electronic Science and Technology of China, Chengdu 610054, China.
*** Corresponding author at: Department of Physics and JILA, University of Colorado, Boulder, CO 80309, United States.
E-mail addresses: junzhao80@163.com (J. Zhao), wjun@uestc.edu.cn (J. Wang), markus.raschke@colorado.edu (M.B. Raschke).

https://doi.org/10.1016/j.infrared.2023.105114
Received 15 December 2023; Received in revised form 25 December 2023; Accepted 28 December 2023
Available online 4 January 2024
1350-4495/© 2023 Published by Elsevier B.V.

amplification is necessary for effective collection. Conventional external circuit amplification, such as preamplifiers and lock-in amplifiers, often sacrifices bandwidth, posing a challenging issue for high-speed detection systems. Therefore, it is crucial to have devices with high internal gain that can amplify the signal without reducing bandwidth. Typical devices with internal gain include photomultiplier tubes (PMTs)[6], optically guided devices with high carrier lifetime, quantum dot resonance tunneling detectors (QD-RTDs)[7], and APD[8]. PMTs offer high gain but operate at high bias voltage and have very low detection efficiency, as well as relatively high dark counts. High-gain optically guided devices sacrifice response time for higher gain, resulting in very low bandwidth. QD-RTD is a novel photon-number-resolving detector, but its operating point is sensitive to light exposure, requiring long-term statistical confirmation of results, which limits its application. Compared to other high-gain devices[9], APDs combine high bandwidth and gain, are easy to fabricate, and can ensure quantum efficiency. Although issues such as dark current and excess noise still need to be addressed, APD offers significant advantages for the detection of extremely weak light.

APD leverage the avalanche effect to amplify the number of charge carriers and produce substantial gain. When photovoltaic devices are exposed to a high reverse bias voltage, a strong electric field forms within the device, this electric field causes charge carriers to gain significant kinetic energy, becoming hot carriers. When the energy of hot charge carriers is low, they interact with impurities and phonons, transferring energy without generating new free charge carriers, thus losing the gain effect. However, when the energy of hot charge carriers surpasses their impact ionization threshold energy, they collide with the lattice, creating electron-hole pairs. These newly generated pairs continue to collide under the influence of an external electric field, leading to the production of a large number of free-charge carriers. Yet, if the electric field is too intense, the impact between hot carriers and the lattice becomes more disorderly, resulting in significant excess noise and rendering the device unsuitable for infrared light detection. At an appropriate voltage, APD achieve substantial gains caused by the avalanche effect of charge carriers. Moreover, a higher external electric field enables the device's free carrier mobility to reach saturation, providing high gain and high bandwidth characteristics. This is particularly beneficial for systems requiring extremely sensitive detectors, such as light detection and ranging (LiDAR), deep space exploration, space optical communication, three-dimensional target imaging, active and passive target detection, atmospheric remote sensing, two-color detection, and camouflage identification in Fig. 1 [10]. CMOS-integrated silicon-based APD have reached a relatively mature stage, with applications in the Mozi quantum communication satellite, as well as in vehicle and airborne LiDAR. However, the use of 905 nm and other bands for silicon LiDAR may pose risks to human eyes. Additionally, silicon APD are unable to detect lower energy infrared photons, such as those in the communication bands 1310 and 1550 nm, mid-wave infrared bands, and long-wave infrared bands. Therefore, achieving

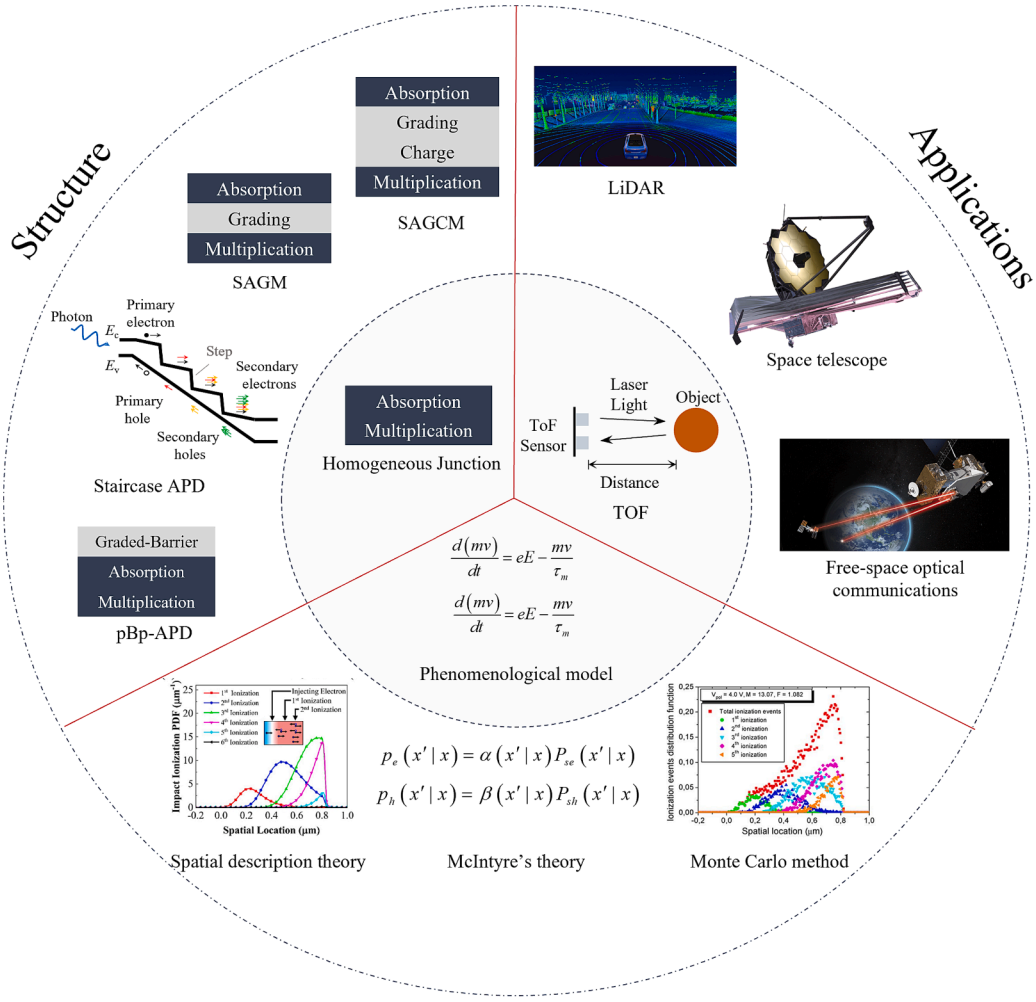


Fig. 1. Theory, Structure, and Applications roadmap for avalanche photon detector technologies.

high-speed detection of weak signals in mid-wave and long-wave infrared is a crucial research direction for third-generation infrared detection systems. In pursuit of achieving higher performance in APD, various novel APD structures have been proposed, building upon traditional APD designs. These include the SAM structure (separated absorption, multiplication)[11], SACM structure (separate absorption, graded, and multiplication)[12], and SAGCM structure (Separate absorption, grading, charge, and multiplication)[13]. To facilitate the improved design and study of these new APD structures, theoretical research has been pivotal. Given the limitations of the classical McIntyre avalanche multiplication model, Rothman introduced a history-dependent avalanche model. Furthermore, the spatial avalanche model proposed by Hu et al. offers a new insight into the simulation of the avalanche process in APDs[14]. Building upon these theoretical advancements, extensive simulations of particle trajectories under mutual interactions have been conducted[15]. Employing the Monte Carlo method, thermal carriers are treated as classical particles, enabling the simulation of their motion trajectories in potential fields and various impact processes to elucidate the thermal carrier dynamics within the system.

This review showcases the current development status and prospects of infrared APDs, delineated into three main sections: III/V family material-based APDs, APDs composed of novel low-dimensional materials, and II/VI family material-based APDs.

2. II/VI family material-based APDs

APDs based on the II-VI family exhibit characteristics such as low excess noise factor, excellent linear gain, and high quantum efficiency. Among them, HgCdTe APDs stand out as a particularly outstanding type of APD, owing to $Hg_{1-x}Cd_xTe$ is a direct bandgap pseudo-binary material with a sphalerite structure, comprising a blend of the semi-metallic material HgTe (E_g = -0.3 eV) and the semiconductor material CdTe (E_g = 1.5 eV). By adjusting the Cd component, the bandgap of HgCdTe can span the entire infrared band. It is a direct bandgap semiconductor with a notably high absorption coefficient in the infrared band, enabling devices with a 5 ~ 10 μm absorption layer to achieve extremely high quantum efficiency (>90 % in the medium and long wavelength band). Its coefficient of thermal expansion is comparable to that of silicon, allowing for the fabrication of large-scale focal plane devices through integration with silicon readout circuits. The material exhibits a high dielectric constant, high electron saturation mobility, and fast response speed. Additionally, HgCdTe material possesses an electron-hole separation coefficient ratio greater than 1 in the three atmospheric windows of short-wave infrared (1–3 μm, SWIR), mid-wave infrared (3–5 μm, MWIR), and long-wave infrared (8–14 μm, LWIR). According to the classical avalanche multiplication noise mechanism, this would be an excellent material for fabricating low-noise APDs[16,17].

2.1. Theory of II/VI family material-based APDs

The avalanche process in narrow bandgap semiconductors, especially in narrow bandgap semiconductors such as HgCdTe that involve strong alloy scattering, is difficult to study directly using current avalanche theory[18–23]. Currently, there is a trend in the development of narrow bandgap semiconductor theory to form specialized theories [10]. For example, Monte Carlo simulation work in France has yielded clear conclusions on alloy scattering[24], and Kinch's work in the United States, based on the quantum mechanical derivation of impact ionization coefficients, has been reported.

In the classical McIntyre avalanche multiplication model, the impact ionization coefficient for electron-hole impacts is solely determined by the electric field at that specific location. However, the electrons produced by just occurring impact ionization have lower energy and cannot directly undergo impact ionization. Therefore, in the history-dependent avalanche model proposed by McIntyre et al. in 1999, the concept of a dead space is introduced to characterize the range within which newly generated electrons do not undergo impact ionization, thus correcting the classical McIntyre model. The modified formula is as follows[25]

$$\begin{aligned} g_e(x) &= \int_x^w [2g_e(x') + g_h(x') + g_o(x')]p_e(x'|x)dx' \\ g_h(x) &= \int_0^x [g_e(x') + 2g_h(x') + g_o(x')]p_h(x'|x)dx' \end{aligned} \tag{1}$$

where $g_e(x)$ and $g_h(x)$ are the net generation rates produced by electron and hole impact ionization, respectively.

In HgCdTe APD, owing to the large hole mass of the heavy hole band, the migration rate of heavy holes in HgCdTe is very low, and the scattering between heavy holes and optical phonons is very severe. The efficiency of holes in obtaining energy from avalanche regions is very low, and most of the energy obtained is dissipated in the form of optical phonons. Light holes have a very small effective mass at the bottom of the band, but because to the influence of spin–orbit splitting bands, the light hole band bends at the position where impact ionization occurs, resulting in a higher effective mass of light holes with higher energy. Unlike heavy and light holes, the effective mass of electrons in HgCdTe is very small, with high mobility and relatively weak scattering with optical phonons. This makes the efficiency of electrons in obtaining energy from the electric field very high, and due to the narrow bandgap of low Cd component HgCdTe materials, electron avalanche is very easy [22,26–28].

The Full-band Monte Carlo simulation evaluates all necessary information regarding carrier-phonon and carrier-carrier interactions from a first-principles perspective, eliminating the need for introducing empirical coupling constants[29]. Derelle et al. utilized Monte Carlo simulations to study HgCdTe APDs and demonstrated single-carrier impact ionization. They conducted a comparative study of the impact of different scattering process combinations on the avalanche phenomenon in HgCdTe[30,31]. Monte Carlo simulations in HgCdTe APDs have demonstrated that the low excess noise factor may stem from the distance traveled by carriers (electrons) before acquiring sufficient energy to trigger new impact ionization events. As shown in Fig. 2 (a-c), The probability of each carrier inducing an impact ionization event depends is contingent upon its preceding interactions, commonly known as the history-dependent theory as proposed by Rothman[31–37]. They derived a comprehensive model for the gain of HgCdTe APDs and applied the history-dependent model to fit gain curves of APDs with varying geometries and cutoff wavelengths. The variable dead space effect significantly influences the excess noise of APDs, and accurate excess noise measurements can facilitate correlated estimations of the non-local impact ionization function. However, the Monte Carlo calculations used by Rothman are not based on quantum mechanical derivations, but instead rely on empirical formulas for impact ionization. In 2021, Hu and Xie et al. proposed the Spatial Description theory based on spatial description realized, for the first time, an analytical model of the avalanche process of narrow-bandgap semiconductors based on quantum mechanics, denoted as Hu-Xie avalanche theory,

$$N^{(m)}(x_0, x_m) = 2^{m-1} g(x_0) P_{se}^{(m)}(x_{m-1}, x_m) \prod_{n=1}^{m-1} \left(1 - P_{se}^{(n)}(x_{n-1}, x_n)\right) \tag{2}$$

where $g(x)$, $P_{se}^{(m)}$ and m are the normalized distribution of the injected nonequilibrium carrier, survival probability, and number of generations of electrons, which also modified the microscopic scattering model proposed by Kinch and F. Ma. Each term in the multiplication represents the probability of the electron does not survive in every previous impact ionization. As shown in Fig. 2 (g-i), the part before the multiplication represents the impact ionization probability of the electron in this round of impact ionization. By analyzing all the possibilities from x_0 to x_m, Hu et al. get the probability of electrons' impact ionization in each start position and end position. Using the Hu-Xie avalanche theory, the

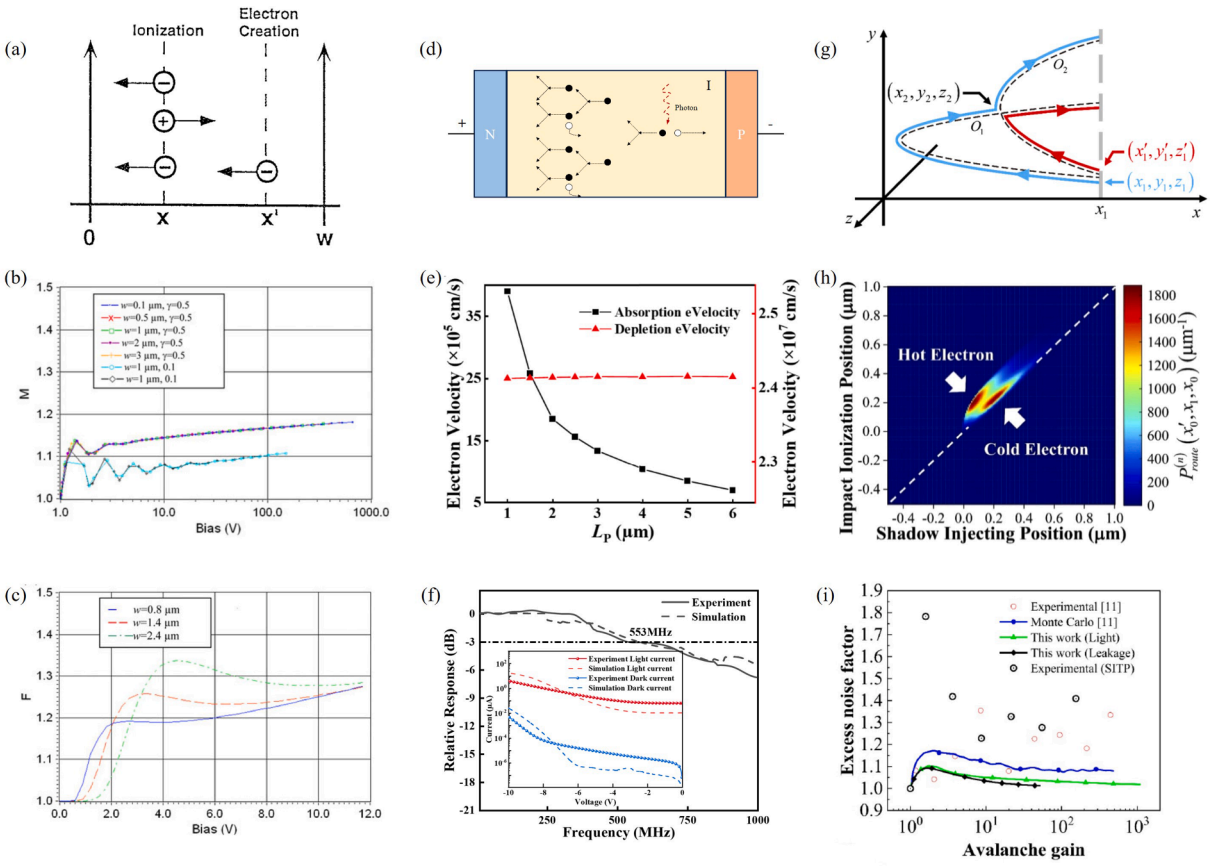


Fig. 2. Theory of II/VI family material-based APDs. (a) Schematic of the spatial notation for electrons. Carriers are created at x' and ionization occurs at x. (b) Excess noise using Shockley's expression for a constant dead-space ratio and the saturation of the impact ionization coefficient. (c) Measured and calculated excess noise using Shockley's expression for the saturation of a variable dead-space ratio and the impact ionization coefficient. (d) Schematic diagram of avalanche excess of charge carriers in APD. (e)Simulated carrier velocities within the absorption and depletion regions. (f) The simulations and experiments characterize the frequency response and current characteristics of the optimized device. (g) The scattering in the pull-back motion starts at x_1. (h) Illustration of shadow area and correction of calculated shadow area. (i) ENF of photocurrent and leakage current.

obtained excess noise suppression mechanism by alloy scattering has been widely accepted by researchers in recent years, and has become the major principle for the design and noise suppression of HgCdTe APDs. [14].

Currently, the MWIR HgCdTe photodetectors at the French CEA-LETI Infrared Laboratory have excess noise factors of less than 1.5 at gains below 1000. Additionally, there are reports, such as the work reported by the American company DRS, showing a significant increase in excess noise factor after a certain voltage. Due to the excellent noise performance of HgCdTe, as well as the different fabrication processes and device preparation methods in different countries, some mechanisms that are not significant in avalanche devices made of other materials are highlighted in HgCdTe photodetectors. Based on the two core indicators of HgCdTe avalanche detectors, gain and excess noise factor, the concepts of shadow region correction and incomplete avalanche model are proposed. The historically dependent avalanche model, with fewer assumptions, extends the classical McIntyre avalanche multiplication theory and was applied to the description of HgCdTe avalanche processes by Kinch et al. in 2011[23,30]. However, due to several overly strong assumptions, it is difficult to use it in conjunction with more accurate impact ionization rates based on quantum mechanics. The Hu-Xie avalanche theory extended the history-dependent avalanche model based on McIntyre's assumptions, combine the influence of shadow region correction and spatial dependence of electrons in avalanche region [14]. In the realms of near-field optical and electrical characterization, a multitude of non-local phenomena manifest. In-depth investigations and characterization of detectors in near-field optics necessitate the support of non-local theories to comprehend the intricacies at the microscopic scale. The Hu-Xie avalanche theory, grounded in spatial description avalanche mechanisms, indicates a new pathway for propelling advancements in near-field optics across domains such as non-local responses in plasmas and infrared phononic metasurface responses. [14].

The bandwidth of HgCdTe is also one of its important device performance characteristics. Despite HgCdTe having a small electron-effective mass and high mobility, a comprehensive analysis of carrier transport mechanisms in these devices is imperative for enhancing their operational speed. As shown in Fig. 2 (d-f), Gu et al. utilized a two-dimensional finite element model to investigate the carrier transport mechanisms under various device structures and bias voltages.[38]. Following a comprehensive assessment of the device's bandwidth characteristics, the structural parameters of the device were optimized, leading to experimental data that aligned with the computational results. This structural refinement notably elevated the device bandwidth from 27.1 to 553 MHz. As elucidated by Li et al., the prevailing mechanisms in the multiplication region at low bias voltage encompass Shockley-Read-Hall (SRH) and trap-assisted tunneling currents[39]. In 2011, Hu et al. proposed the widely accepted model of trap assisted tunneling in narrow band gap materials,

$$I_{tat} = -A\frac{\pi^2 q^2 N_t m_e^* M^2 (V_{bi} - V_d)}{h^3 E_g - E_t}\exp\left(-\frac{\sqrt{3}E_g^2 F(a)}{8\sqrt{2}qPE}\right) \quad (3)$$

where

$$F(a) = \frac{\pi}{2} + \sin^{-1}(1-2a) + 2(1-2a)\sqrt{a(1-a)} \quad (4)$$

and $a = E_t/E_g$, the analysis theory of trap-assisted tunneling provides a theoretical foundation for mitigating trap-assisted tunneling currents. Building upon this theory, a theoretical model known as Resistance-Voltage has been proposed.

$$R_{\text{fit}} = \left(1/R_{\text{diff}} + 1/R_{\text{gr}} + 1/R_{\text{tat}} + 1/R_{\text{bbt}}\right)^{-1} + R_{\text{s}} \quad (5)$$

In this model, the algorithm is to minimize the function value of

$$F = \Sigma_{i=1}^{N}[\log(R_{\text{fit}}(V_{\text{di}})) - \log(R_{\text{exp}}(V_{\text{di}}))]^2. \quad (6)$$

which plays a guiding role in the dark current analysis in avalanche devices of narrow band gap materials[40]. At high bias voltage, the dark current is primarily influenced by interband tunneling and avalanche currents. Whether it is ion-implanted planar junction HgCdTe APDs or in-situ doped mesa junction HgCdTe APDs, the key to improving device performance lies in the lower doping concentration within the multiplication region. For LWIR HgCdTe APDs, Wang et al. unveiled the anomalous non-equilibrium state induced by deep level defects with the high-resolution in situ characterization method, which improved the spatial resolution from the traditionally reported 2 μm to 0.6 μm[41]. This work pioneered the characterization with spatiotemporal resolution to reveal the impact of non-equilibrium states on carrier transport process and performance of the detector[41].

2.2. New structure of II/VI family material-based APDs

The traditional PIN-structured HgCdTe APD leads to an increase in dark current when a few charge carriers are injected into the avalanche region. Therefore, Li et al. proposed a dual avalanche structure to suppress dark current. This innovative design achieves high gain and low dark current by incorporating a barrier layer within the gradient-doped absorption region. The barrier layer effectively impedes the influx of dark carriers originating from relatively high doping contact or absorption layers, which stem from material defects such as traps or dislocations[42,43].

In 2006, DRS introduced cylindrical "p-around-n" front-illuminated $n^+/n^-/p$ geometric structures in APD[44], facilitating efficient electron injection into the gain region. These devices demonstrate a consistent exponential gain voltage characteristic. In 2007, CEA-LETI conducted a comprehensive set of characterizations on back-illuminated MWIR HgCdTe APD test arrays grown using MBE,

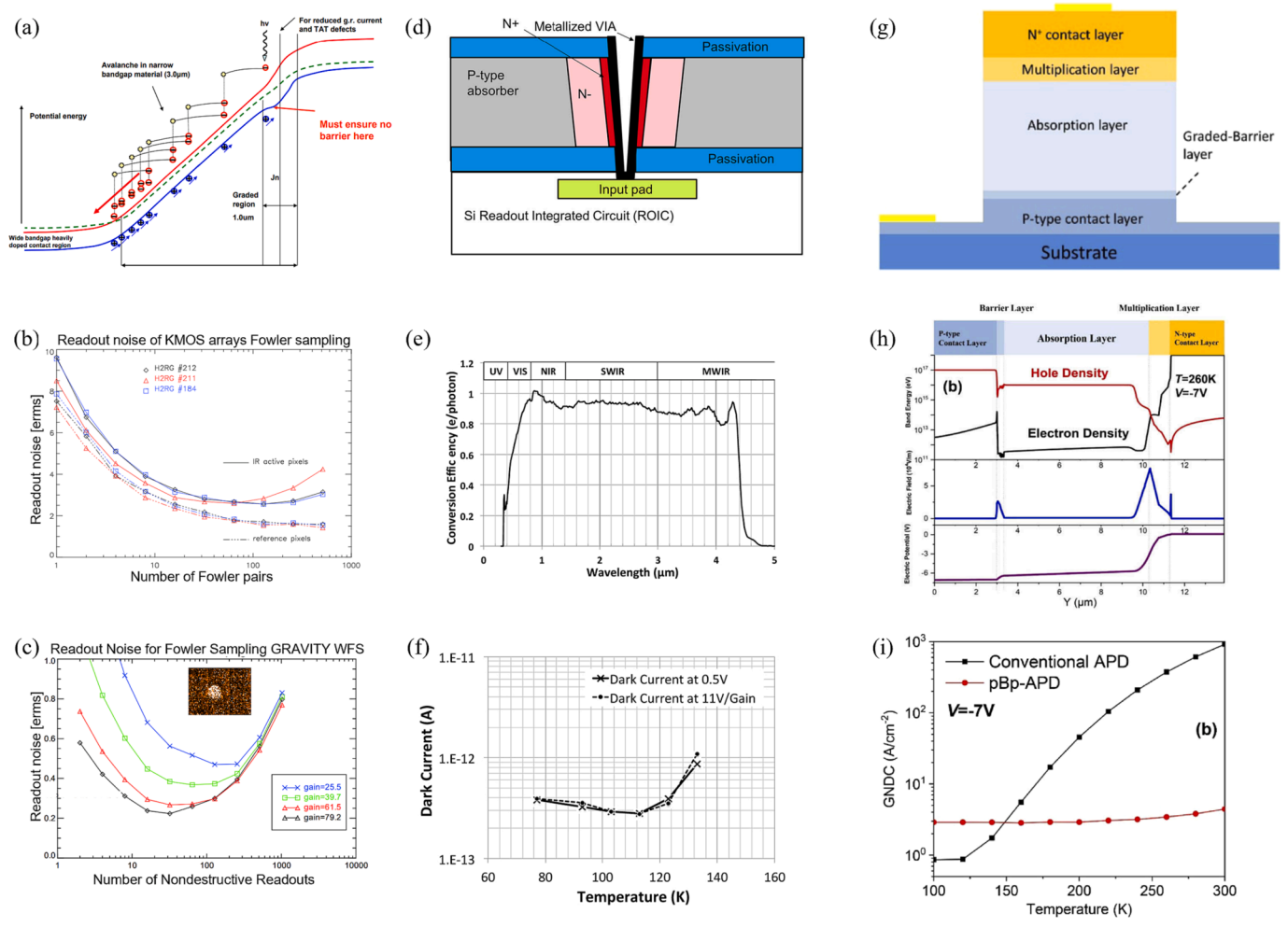


Fig. 3. New Structure of II/VI family material-based APDs (a) Band diagram of MOCVD heterostructure APD array. The junction on the right side and wide bandgap in the absorber region. At small bias voltages narrow bandgap in the gain region for maximum APD gain [48]. (b) Comparison of the persistence of 4 Hawaii-2RG arrays. (c) Presentation of the measured and calculated excess noise utilizing Shockley's expression for the saturation of the impact ionization coefficient and a variable dead-space ratio. (d) Schematic illustration of the high-density vertical integration photodiode (HDVIP) or loop-hole APDs, as utilized by DRS [33]. (e) Spectral response of a 4.3 μm cut-off HDVIP HgCdTe APD [49].(f) Gain-normalized dark current (GNDC) of the HgCdTe APD at 0.5 and 11 V APD bias voltages divided by the APD gain. (g) Schematic of the simulated pBp-APD. (h) At −7 V, simulated vertical distributions of carrier densities, electric field, and electric potential for pBp-APD. (i) GNDC characteristics of pBp-APD and conventional APD.

including excess noise, gain, dark current, and pulse response[45]. These APDs achieved a high avalanche gain of $M = 5300$ with a low noise factor $F = 1.0–1.3$. Additionally, in 2010, DEFIR developed two dedicated e-APD ROICs with a resolution of 320 × 256 and a pitch of 30 μm[46]. The initial characterization of the 3D e-APD-FPA for multi-mode active–passive imaging demonstrated spatial and temporal resolution exceeding 11 cm in a single measurement, meeting most requirements for real-time 3D imaging. In 2012, Sofradir, in collaboration with CEA-LETI, fabricated MWIR cutoff wavelength APDs on and between wafers, demonstrating high gain and low dispersion[47]. In certain diode structures, avalanche gains exceeding 10,000 were observed, further affirming the stability of HgCdTe single-carrier multiplication and underscoring the suitability of Sofradir's process flow for APD manufacturing.

As depicted in Fig. 3(a), using metalorganic chemical vapor deposition (MOCVD), Leonardo has recently grown hetero-structure architectures[48]. In these configurations, CdTe and HgCd have been alternatively grown by Leonardo using MOCVD, with a wide-band gap buffer layer constraining the spectral response at the short-wavelength end to $\lambda > 1.3$ μm. The absorption layer exhibits a cutoff wavelength of $\lambda_c = 2.6$ μm. The absorber effectively segregates carriers from surface states by expanding the bandgap around the periphery of absorber. The absorption region and the gain region are uncoupled, enabling independent optimization. The narrow bandgap of the N-type gain region is tailored to achieve high gain. The primary limitation of this APD appears to be the slower response time at low operating temperatures. In 2017, SUN et al. reported the characterization results of HgCdTe APD arrays developed for infrared laser radar using HDVIP technology[49]. By adjusting the APD gain setting, the detector achieved over 5 orders of magnitude with a non-uniform fixed APD gain. They served as precursors for space-based laser radar and have been successfully applied to airborne CO_2 and CH_4 integrated path differential absorption (IPDA) laser radar.

The emergence of various novel structures presents a viable approach to enhance the performance of high sensitivity detector. By suppressing detrimental local fields within the device and controlling beneficial localized fields[50], advancements in device performance can be achieved. Hu et al. introduced high-resolution in situ characterization method for the "localized field" photocurrent[41,51]. Furthermore, their design of a nanoscale probe sensitive to minority carriers and its near-field enhancement technique enables optical and electrical resolutions at the nanometer scale[51]. This technique significantly propels the advancement of surface-localized field characterization for high sensitivity detector, establishing a robust foundation for the non-local characterization of near-field optics in high sensitivity detector[51]. This near-field photocurrent characterization technique significantly advances the comprehension of material properties and the development of optimization techniques for device structures. This pioneering work[51] has led numerous subsequent studies in the development of new highly sensitive detectors[52–54]. Moreover, it has played a decisive role in elucidating the microscopic mechanisms underlying their photoelectric response[52–54].

In 2020, He et al. applied the pBp structure to HgCdTe APD. As shown in Fig. 3 (g), Through the incorporation of a barrier layer structure in the APD, leading to effective suppression of dark current during the avalanche process, particularly with increasing temperature[55,56]. The guard rings can regulate the local electric field, reduce dark current, and prevent pre-breakdown for APD devices. Introducing a guard ring design effectively mitigates the dark current primarily caused by the surface localized electric field[57]. HgCdTe APDs with guard rings demonstrate higher gain and smaller noise currents compared to devices without guard rings. Importantly, the dark current characteristics of simulated HgCdTe APDs provide insights into the origin of excess noise effects[57]. In addition to the guard ring structure, a photon-trapping architecture is designed to enhance the absorption of infrared photodiodes by utilizing the skin effect of metals[58]. This design provides a new approach for large-size, low dark current focal plane array APDs with small pixels[59].

Dark current is a crucial factor in the design of new structures [60–63]. From the measurement of Resistance-Voltage curves across a wide range of voltage and temperature, four temperature-dependent crucial parameters concerning the electron lifetime in the p-region, the effective lifetime in the depletion region, the relative energy position of trap levels, and the trap density in the depletion region have been extracted. In 2010, Hu et al. proposed [64,65] and improved [40] a temperature-voltage model for dark current of HgCdTe infrared detectors, which laid the foundation for today's dark current analysis based on wide-range temperature-based characterization. With over 10 years of development, this research paradigm has been widely adopted by the infrared flagship institutions (such as Raytheon from USA, CEA-LETI from France, SITP from China, and etc.), and has become an important technical method in the design and development of the advanced infrared devices in recent years[39,66–71].

3. APDs composed of novel low-dimensional materials

Low-dimensional materials are classified into 2D (van der Waals, vdW) materials, 1D (quantum nanowires), and 0D (quantum dots) each manifesting unique optical and electrical properties that set them apart from 3D materials, thus providing new avenues for the design of advanced APDs[60,72–77]. In this context, we aim to present an overview of 2D materials. The unique properties of 2D materials enable their application in APD. In low-dimensional materials, atoms with layers being connected by weak vdW interactions, within the same plane are linked by ionic or covalent bonds. Due to the relatively loose interlayer connections, two-dimensional materials can be manufactured using the mechanical exfoliation method. Furthermore, the presence of weak vdW bonds facilitates the relatively easy formation of heterostructures by combining different low-dimension materials. Many APDs have already been implemented using nanowires and two-dimensional materials. However, there is limited detailed theoretical research on the avalanche mechanism within low-dimension photodetectors[73,78–80].

3.1. Theory of low-dimensional materials-based APD

Taking graphene as an example, consists of a two-dimensional hexagonal structure of carbon atoms, showcasing distinctive electrical properties. The conduction band touches the valence band, rendering graphene a semimetal with exceptional electronic characteristics.[81].

In 2019, Michael et al. conducted a theoretical investigation into the interaction between band structure and carrier dynamics in a model system of quasi-two-dimensional narrow bandgap material. Fig. 4 presents a quantitative study of the carrier and band dynamics in graphene, showcasing various effects following ultra-short optical excitation in Fig. 4(a), and subsequently in Fig. 4(b-d). The coherent phonons induce band dynamics leading to a decrease in the band gap and an alteration in the band curvature[82].

In 2007, Rana et al. conducted a study examining the electron-hole generation and recombination rates associated with Coulomb scattering (including Auger recombination and impact ionization) in graphene[83]. Their research indicated that in graphene, the electron-hole recombination time can exceed 1 ps at all temperatures when the electron-hole density is less than 10^{12} cm^{-2}. Compared to most ordinary semiconductors, the Auger recombination rate in zero-bandgap graphene is generally faster. Tani et al. first observed large terahertz-induced near-infrared transparency in graphene[84]. By conducting analysis, they showcased the occurrence of a carrier multiplication process in graphene induced by high fields and ultra-short terahertz pulses. The correlation between the rise in charge density and the peak terahertz field strength in graphene indicates the involvement of interband impact ionization mechanisms. The impact ionization process can suppress the emission of optical phonons by diminishing the kinetic

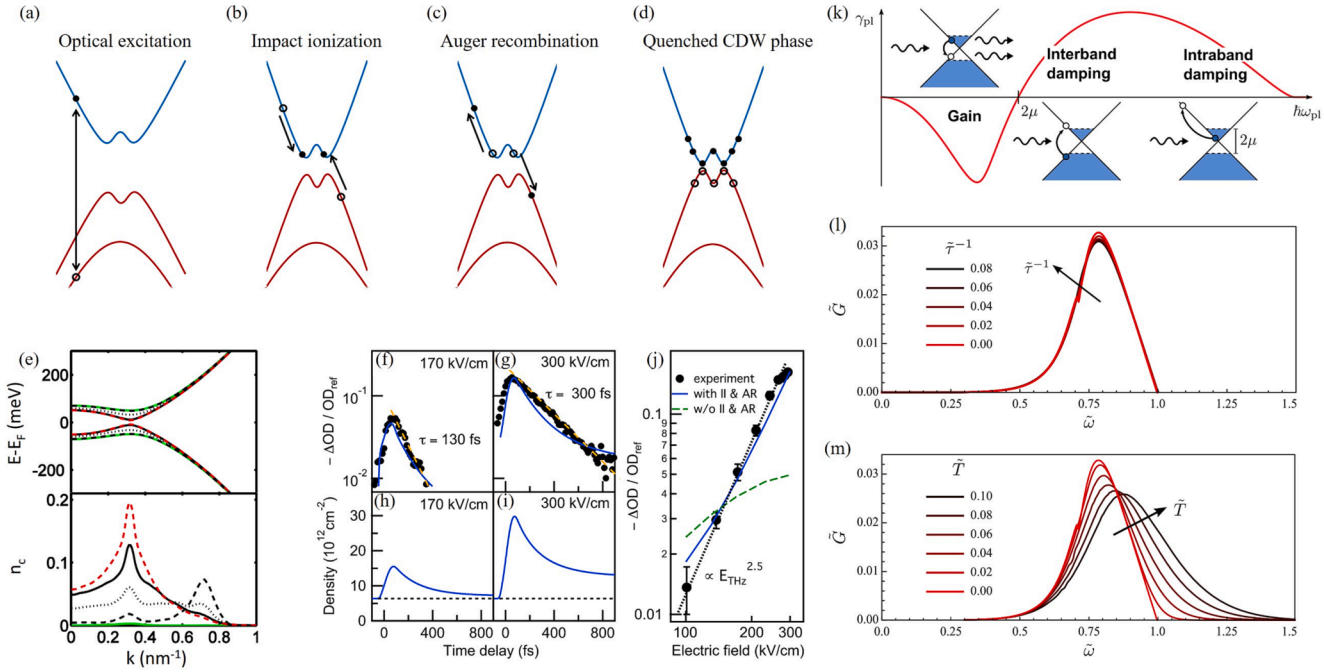


Fig. 4. New avalanche theory of low-dimensional materials-based APD. Schematic depiction of (a) the optical excitation, (b) impact ionization phenomena, (c) Auger recombination phenomena, and (d) the near-equilibrium state in the rapidly cooled charge density wave (CDW) phase. The valence bands are represented by red bands, while the conduction band is denoted by the blue band. (e) Depicts band dynamics (top) and carrier distribution in the conduction band (bottom). The normalized differential optical density induced by THz, plotted against time delay for peak electric fields of (f) 170 kV/cm and (g) 300 kV/cm, showcasing both experimental data (circle) and simulated results (solid line). Through a single exponential fit (dashed line), the relaxation time is determined. Panels (h) and (i) depict the calculated carrier density as a function of time delay, with dashed lines representing the initial carrier density. Additionally, panel (j) illustrates the THz-induced transparency of graphene as a function of peak electric field, showcasing experimental data (filled circle) and simulations (solid and dashed lines). Notably, the experimental results adhere to a power law with an exponent of 2.5 (dotted line). Panel (k) presents the plasmon decay rate over plasmon energy for inverted intrinsic graphene, highlighting the impact of impact loss and temperature on the plasmon gain spectra. Furthermore, panels (l) and (m) display the plasmon gain spectra for m = 0 under varying impact loss rates and temperatures, respectively. (For interpretation of the references to color in this figure legend, the reader is referred to the web version of this article.)

energy of carriers, thereby promoting effective carrier transport and suppressing current saturation. Oladyshkin et al. in 2017 used P-doped graphene with an initial Fermi energy of approximately 200 meV and detected photons in the range of 2.0–3.5 eV[85]. With the increase in terahertz field intensity, the photon energy remained constant, while the number of emitted photons increased by several tens, signifying that the multiplication of electron-hole pairs in graphene is prompted by alterations in the external field. In 2015, Page et al. demonstrated that graphene can support gainful plasmon polaritons under realistic conditions. Through a comprehensive exploration of non-equilibrium polarization theory, they systematically examined the influences of doping, impact losses, and temperature on the dispersion of plasmons and the gain/loss spectra[86]. While doping and temperature can shape the emission spectrum, impact losses result in a proportional reduction in gain corresponding to the impact rate. The frequency dispersion curve, however, remains resilient against impact losses and temperature but is notably influenced by doping. Upon reaching a critical value of particle/hole chemical potential imbalance, the dispersion of plasmon polaritons encounters a singularity and undergoes a transformation. These findings suggest the feasibility of plasmon amplification under realistic assumptions of impact losses and temperature. Based on the aforementioned research, the theoretical investigation of avalanche processes in current low-dimensional materials is rapidly advancing. This includes exploring various doping effects and the impact of temperature on collision ionization within low-dimensional materials. Additionally, there is a focus on how the unique band structures of two-dimensional materials affect carrier mobility. Future endeavors will necessitate a more systematic study and development concerning carrier collisions and scattering phenomena within low-dimensional materials.

3.2. New structure of low-dimensional materials-based APD

Based on studying the mechanism of low-dimensional materials, designing the structure of APD devices composed of 2D materials also presents a significant challenge.

Low-dimensional materials provide an excellent pathway for achieving detectors with remarkably low capacitance and heightened sensitivity. This is partly due to the small junction area enabled by the characteristics of low-dimensional materials. Moreover, the electrostatic shielding of charges in low-dimensional structures substantially enlarges the space-charge region beyond the depletion width observed in three-dimensional materials, leading to a decrease in junction capacitance. Fig. 5(a) illustrates the advantages of utilizing low-dimensional materials for optoelectronic detection: reducing the thickness of 2D materials or the diameter of nanowires (1D) can significantly improve sensitivity. The sensitivity comparison of photodetectors based on various low-dimensional materials in Fig. 5 (b) underscores the direct practicality of this approach. Furthermore, the sensitivity, expressed by multiplying NEPh by internal quantum efficiency [87].

In 2006, Yang et al. synthesized axially modulated doped PIN silicon nanowires with uniform diameter and single-crystal structure[89]. Spatially resolved photocurrent measurements demonstrating the functionality of individual PIN nanowires as avalanche photodiodes. Their study of Si nanowires laid the foundation for investigating impact ionization processes in quasi-one-dimensional semiconductor systems. In 2017, Jain et al. proposed a spectral-tunable absorption InP/InAsP nanowire-based SAM APD at 1.55 μm[90]. To achieve spatially SAM in heterostructure nanowires, the bandgap in the absorption region transitions from InP to InAsP. The primary achievement of this study was the

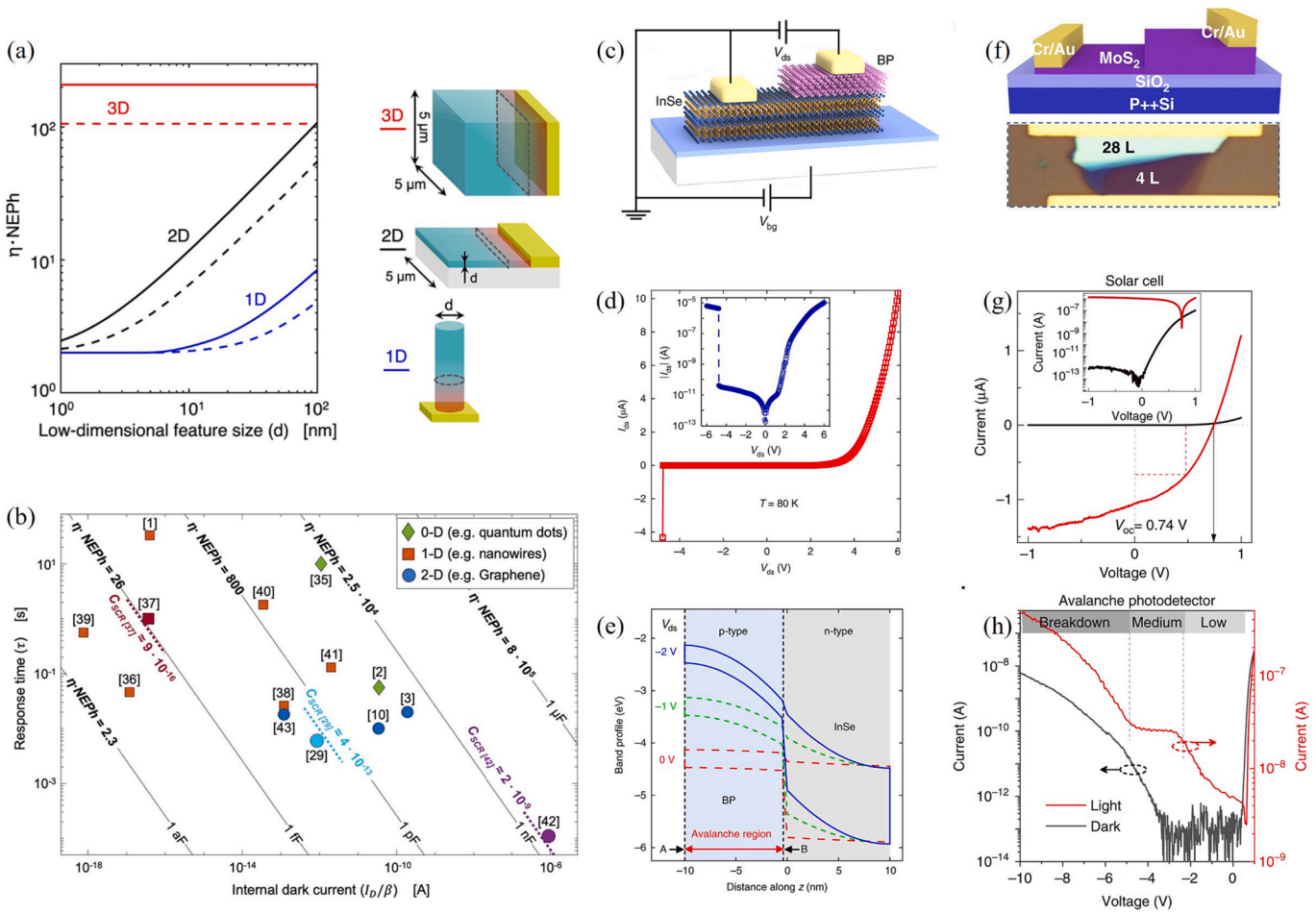


Fig. 5. New structure of low-dimensional materials-based APD. (a) Comparison of the sensitivity of low-dimensional photodetectors (1D and 2D) to bulk (3D), expressed as noise equivalent photon (NEPh) multiplied by internal quantum efficiency, as a function of the low-dimensional feature size d. The figure depicts the sensitivity at 300 K with solid lines, and at 77 K with dashed line [87]. (b) Detectors based on 0D (diamonds), 1D (squares), and 2D (circles) materials, showcasing the response time and internal dark current. [87]. (c) Schematic of the graphene InSe/BP[88]. (d) I_{ds}-V_{ds} characteristic of an InSe/BP avalanche device on a linear scale. (e) At bias voltages of 0, −1, and −2 V, the calculated band profiles are depicted. The colored region (BP) signifies the occurrence of impact ionization, with A and B denoting the surfaces of BP connected to the metal and InSe, respectively. (f) Optical-microscope images and a schematic representation of a layered PN junction on a MoS_2 flake. (g) The IV curves of the MoS_2 layer junction under dark and photo-excited conditions. (h) IV curves under low temperature conditions (~100 K) in both dark and photo-excited states.

inaugural demonstration that selective excitation of the absorption region using photons and electrons consistently yielded multiplication gains of up to 12. These devices represent promising candidates for the future advancement of array-based SAM APD utilizing nanowires. In 2015, Lei et al. achieved avalanche gain and improved the device response of a two-dimensional InSe material-based photodetector by utilizing a large Schottky barrier between InSe and Al electrodes[91]. Their device enhanced external quantum efficiency while maintaining low dark current and fast response time. Additionally, the use of plasma-enhanced Al nanodisks improved the device's performance, a processing method that can also be extended to photodetectors made from other 2D materials. In 2022, Liu et al. showcased a high-performance black phosphorus APD operating at two wavelengths, based on a Si hybrid plasmonic waveguide[92]. This structure simultaneously enhances light absorption in black phosphorus while reducing carrier transit time. Due to the avalanche multiplication process in black phosphorus, this waveguide APD exhibited high responsivity of 66 A/W (optical power of 2.9 μW) at 1.55 μm and 125 A/W (optical power of 1.4 μW) at 1.95 μm, with a measured 3 dB bandwidth of 1.05 GHz, this high-performance Si/BP waveguide APD presents a promising option for optical sensing, imaging, and communication applications at 1.55/1.95 μm and even longer wavelengths, surpassing those reported for high-gain photodetectors based on 2D materials by at least three orders of magnitude. In the near-infrared region, Liu et al. integrated silicon with macroscopic assembled graphene nanofilms (nMAG), demonstrating a high-performance Schottky diode with a wide spectral range (1342–1870 nm), high responsivity, and high speed. The response of nMAG in the IR region is attributed to its high light absorption, low work function, and long carrier lifetime, while the high response of nMAG/Si is influenced by the avalanche multiplication effect in Si.[93]. In 2014, Hu et al. proposed a novel unipolar barrier design to suppress the crosstalk in two-color infrared photodetectors[59]. Based on the interesting "localized field" energy band design with the groove aperture for the long-wavelength detection component, Hu et al. correlated the microscopic response mechanism and the figure of merit of device-level 128 × 128 two-color infrared photodetectors for the first time, laying the foundation for the proposal of the stacked layer mid-wavelength/long-wavelength two-color detection structure[59]. Low-dimensional materials have advantages in obtaining stacked layer structures, and similar stacked layer structures for multi-color detection are also the focus of current research[94–96]. The proposed design has become an important basis for Raytheon to develop low crosstalk two-color infrared photodetectors[59,97]. In 2021, A novel captivating van der Waals-based unipolar barrier heterostructure to suppress the dark current in

detectors designed by Hu Group [94]. By addressing concerns related to lattice and band mismatch, the van der Waals infrared detectors exhibit a high detectivity even when operated at room temperature. This work provides not only an impactful idea for the suppression of avalanche gain normalized dark current density (GNDCD), but also a new direction for the development of room temperature MWIR and LWIR APDs especially based on low-dimensional materials.

In 2019, Gao and colleagues reported the detection of ballistic avalanche phenomena in vertically integrated InSe/black phosphorus (BP) heterostructures scaled to sub-mean free path (MFP). This discovery opens the door to the development of APD sensitive to MWIR light (4 μm wavelength)[88]. These APD devices exhibit a low noise figure, low avalanche threshold (<1 V), and a distinctive density spectral shape. This breakthrough paves the way for the creation of advanced photodetectors capable of efficient carrier manipulation at the nanoscale. In 2022, a novel structure based on MoS_2, termed the "layer PN junction [98]" was reported. With increasing layer thickness, the electrical conductivity of molybdenum disulfide flakes undergoes self-regulation from electron-to-hole conduction. This implies the ability to construct a uniform PN junction with record-high rectification ratios (>10^5) and low cutoff currents (<1 pA) at the size/precision of a single layer[98]. This layer PN junction has been proved to be an effective solution for the long-standing issue of defects and incomplete depletion caused by heterostructure assembly in low-dimensional materials-based APD. Recently, Wang et al. proposed an ingenious sandwiched heterostructure, which brought new ideas to the solutions of the incomplete depletion for low-dimensional PN junction and pointed out a new direction for the low-dimensional APD[99]. This fully depleted self-aligned vdW heterostructure sandwiched between two electrodes exhibits competitive performance, including an ultra-wide effective detection range, which is twice that of state-of-the-art MWIR photodetectors[99]. Following this pioneering work, photodetectors with fully depleted structures have sprung up[100,101]. The vdW heterostructures of graphene and transition metal dichalcogenides exhibit significant responses to optical excitation but have been unable to achieve single-photon resolution photon counting. Roy et al. demonstrated the sensitivity of bilayer graphene (BLG) and molybdenum disulfide (MoS_2) combined devices to photon counting[42]. At an operating temperature of 80 K, the resulting devices were able to unambiguously determine the emission statistics of the light source with single-photon resolution, dark count rate of 0.07 Hz, and a linear dynamic range of ≈ 40 dB. The device leverages the tunable bandgap in BLG to decrease channel current, consequently reducing the noise level. On the path to exploring ultrafast, high-performance detectors, a novel uncooled MWIR vdW-on-HgCdTe photodetector has been developed[102]. By combining high-mobility graphene with highly absorption HgCdTe, the device maximizes the advantages of these two materials, resulting in high detectivity and a response speed twice that of commercial room-temperature HgCdTe

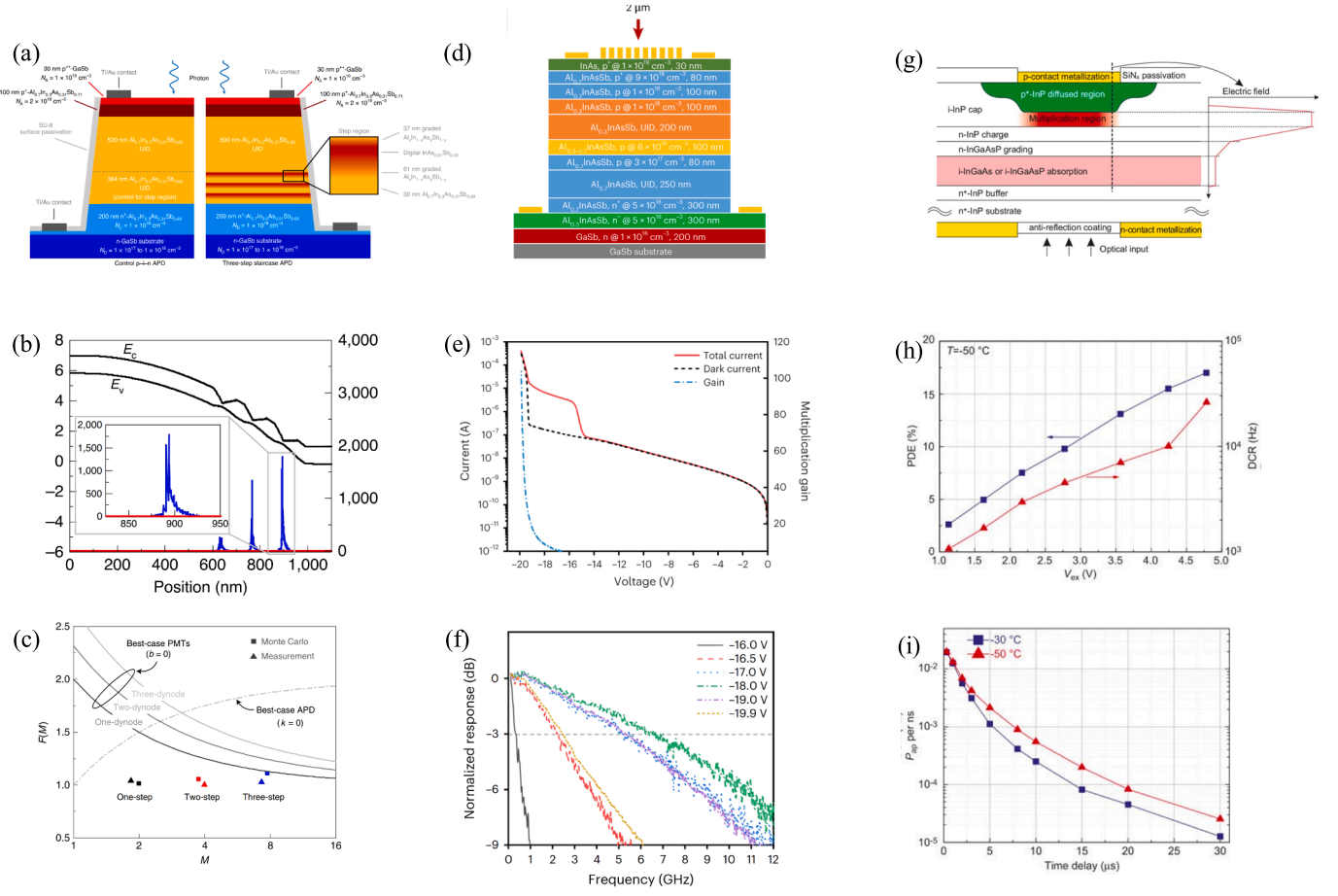


Fig. 6. New Structure of III/V family material-based APDs. (a) Step-free control PIN APD (left) and three-step AlInAsSb staircase APD (right). (b) Simulated band structures for three-step AlInAsSb staircase APDs operating at −4, −5, and −6 V, respectively, to achieve ~ 2^N gain are depicted. The modeled impact ionization events, in the step regions primarily initiated by electrons (blue), indicate the prevalence of electron-only initiated impact ionization events over hole-initiated events (red) (c) Measured and simulated F(M) for one-step, two-step, and three-step staircase APDs. (d) Photon-trapping SACM APD structure. (e) Measured current–voltage and gain curves of a 100-μm-diameter device at room temperature are presented. Additionally, the frequency response of the SACM APD with dimensions of 10 × 35 μm^2 is depicted. (g) SAGCM structure of InGaAs/InP SPAD. (h) Experimental characterization of an InGaAs/InP SPAD, illustrating the PDE and DCR as a function of Vex at −50 ℃. (i) Normalized parameter of Pap per nanosecond as a function of time delay between two gates, with PDE set at 10 % at temperatures of −30 ℃ and −50 ℃, respectively[104]. (For interpretation of the references to color in this figure legend, the reader is referred to the web version of this article.)

heterojunction APDs. This design[102] offers a solution for integrating low-dimensional materials with traditional counterparts in the future.

4. III/V family material-based APDs

Since its discovery, APDs have undergone various structural changes. Numerous attempts have been made to reduce dark current and increase avalanche gain. In addition to exploring various novel low-dimensional materials, the mature application of III-V compound APDs initially adopted a PIN-type homojunction structure[103–109].

In 1982, Capasso and colleagues introduced the concept of staircase avalanche photodiodes. As shown in Fig. 6 (a-c), in 2021, March et al. demonstrated a three-step gain scaling, where the measured results exhibited the expected proportionality between 2^N and the staircase steps N[110]. Furthermore, unexpected low-noise characteristics were observed compared to photomultiplier tubes, stemming from the reduced uncertainty in each step's impact ionization. These detectors can be utilized as room-temperature amplifying detectors and may ultimately surpass PMTs in sensitivity. Staircase APDs with only a few steps have already emerged as direct competitors to traditional APDs.

Traditional MWIR infrared detectors, such as HgCdTe, require low operating temperatures to mitigate excessive dark currents. To address this issue, Chen et al. introduced a photon-trapping structure-based avalanche photodiode design utilizing AlInAsSb, offering the advantages of high quantum efficiency and low dark current in Fig. 6 (d-f) [111]. When compared to state-of-the-art HgCdTe APDs, the dark current is reduced by three orders of magnitude. Furthermore, the thinner absorption layer design enhances the bandwidth, with frequency response measurements indicating a maximum bandwidth of approximately 7 GHz and a gain-bandwidth product exceeding 200 GHz.

In 1992, Liu et al. introduced an APD with SAM in InGaAs/InP. The device incorporated double-diffused floating guard-ring structures to prevent edge breakdown and markedly reduce the electric field at the semiconductor/insulator interface. The study delved into the operational mechanism and optimized design of APDs based on a two-dimensional device model[112]. In 2001, Xiao et al. conducted a systematic study of the temperature-dependent performance characteristics of InP/InGaAs SAGCM APD. This study encompassed an analysis of gain, breakdown voltage, 3 dB bandwidth, gain-bandwidth product, and excess noise factor, employing a simplified time-domain simulation method[113]. Duan et al. proposed a SACM (InGaAs-InAlAs) APD in 2005, which achieved better control of impact ionization by implementing an electric field gradient within the multiplication region. Crucial for high-bit-rate single-photon applications, are short dead times [114]. In 2009, Dixon reported InGaAs avalanche photodiodes with a gate-controlled Geiger mode at 1.036 GHz and a dead time of only 1.93 ns. In the same year, InGaAs/InP APDs achieved short gate pulses and optimized self-differencing circuits at the 1550 nm communication band, significantly enhancing the APD performance[115]. Widely employed in photon-starved optical communication systems, SAGCM APDs exhibit significant photocurrent gain. A comprehensive analysis of the dark current in SAGCM InGaAs-InP APDs with varying multiplication layer thicknesses was undertaken, addressing the influence of diffusion, generation-recombination, tunneling, and multiplication processes on the total leakage current. Williams designed a multi-stage InGaAs APD, which exhibits lower excess noise and dark current [116]. The performance improves with an increasing number of stages. This structural hierarchy enhances the electron-initiated impact ionization rate and suppresses the hole-initiated ionization rate under low-gain conditions.

5. Conclusions

This review presents a comprehensive exploration of the latest developments in the realm of infrared avalanche photodetectors, with a specific focus on the integration of II-VI, III-V, and emerging low-dimensional materials. Infrared APDs find wide applications in fields such as LiDAR, deep space exploration, space optical communication, three-dimensional target imaging, active and passive target detection, atmospheric remote sensing, thus demanding detectors with high sensitivity and responsiveness. APDs from the II-VI family, represented by HgCdTe, hold great potential in the infrared spectrum, but their application is constrained by the requirement for low-temperature cooling. Research on HgCdTe APDs has already established a theoretical framework rooted in quantum mechanics, providing a solid foundation for better understanding and optimizing device design. As theoretical research progresses, it points the way for the structural design of higher-performance HgCdTe detectors. Some high-performance low-dimensional materials offer a new approach for the development of traditional APDs, and low-dimensional materials can be rapidly developed, validated, and manufactured to meet various application scenarios. While there are some theoretical studies on the impact ionization of graphene, a systematic study of avalanche theory for low-dimensional material APDs is still lacking, necessitating further theoretical research to drive the development of high-performance low-dimensional material detectors. Low-dimensional material APDs are still in their infancy, and the mature technology of III-V family APDs can provide insights for the design of other material APDs. With the support of theoretical research, the design of new materials and novel-structured APDs is driving APDs towards higher performance. It is believed that the integration of low-dimensional materials with traditional materials offers a new direction for the development of devices with high sensitivity and low excess noise factor.

CRediT authorship contribution statement

Shuning Liu: Writing – original draft. **Qi Han:** Data curation. **Wenjin Luo:** Writing – review & editing, Conceptualization. **Wen Lei:** Methodology. **Jun Zhao:** Supervision. **Jun Wang:** Supervision. **Yadong Jiang:** Supervision. **Markus B. Raschke:** Supervision.

Declaration of competing interest

The authors declare that they have no known competing financial interests or personal relationships that could have appeared to influence the work reported in this paper.

Data availability

No data was used for the research described in the article.

Acknowledgments

This work was supported by National Key Research and Development Program of China (Grant No. 2023YFB3611401) and National Natural Science Foundation of China (No. 62175026, 61922022).

References

[1] B. Levine, R. Malik, J. Walker, K. Choi, C. Bethea, D. Kleinman, J. Vandenberg, Strong 8.2 μm infrared intersubband absorption in doped GaAs/AlAs quantum well waveguides, Appl. Phys. Lett. 50 (1987) 273–275, https://doi.org/10.1063/1.98223.

[2] L. West, S. Eglash, First observation of an extremely large-dipole infrared transition within the conduction band of a GaAs quantum well, Appl. Phys. Lett. 46 (1985) 1156–1158, https://doi.org/10.1063/1.95742.

[3] W. Hu, Q. Li, X. Chen, W. Lu, Recent progress on advanced infrared photodetectors, Acta Phys. Sin. 68 (2019) 120701, https://doi.org/10.7498/aps.68.20190281.

[4] A. Ouerghi, M. Ridene, A. Balan, R. Belkhou, A. Barbier, N. Gogneau, M. Portail, A. Michon, S. Latil, P. Jegou, A. Shukla, Sharp interface in epitaxial graphene layers on 3 C -SiC(100)/Si(100) wafers, Phys. Rev. B. 83 (2011) 205429, https://doi.org/10.1103/PhysRevB.83.205429.

[5] A. Ouerghi, A. Balan, C. Castelli, M. Picher, R. Belkhou, M. Eddrief, M.G. Silly, M. Marangolo, A. Shukla, F. Sirotti, Epitaxial graphene on single domain 3C-SiC

(100) thin films grown on off-axis Si(100), Appl. Phys. Lett. 101 (2012) 021603, https://doi.org/10.1063/1.4734396.
[6] R. Foord, R. Jones, C.J. Oliver, E.R. Pike, The Use of Photomultiplier Tubes for Photon Counting, Appl. Opt. 8 (1969) 1975–1989, https://doi.org/10.1364/AO.8.001975.
[7] W. Lu, Z. Ji, L. Pfeiffer, K.W. West, A.J. Rimberg, Real-time detection of electron tunnelling in a quantum dot, Nature 423 (2003) 422–425, https://doi.org/10.1038/nature01642.
[8] F. Capasso, Band-Gap Engineering: From Physics and Materials to New Semiconductor Devices, Science 235 (1987) 172–176, https://doi.org/10.1126/science.235.4785.172.
[9] W. Luo, Q. Weng, M. Long, P. Wang, F. Gong, H. Fang, M. Luo, W. Wang, Z. Wang, D. Zheng, W. Hu, X. Chen, W. Lu, Room-Temperature Single-Photon Detector Based on Single Nanowire, Nano Lett. 18 (2018) 5439–5445, https://doi.org/10.1021/acs.nanolett.8b01795.
[10] W. Hu, X. Chen, Z. Ye, C. Lin, F. Yin, W. Lu, Numerical analysis of two-color HgCdTe infrared photovoltaic heterostructure detector, Opt. Quantum Electron. 41 (2009) 699–704, https://doi.org/10.1007/s11082-010-9381-3.
[11] N. Susa, H. Nakagome, H. Ando, H. Kanbe, Characteristics in InGaAs/InP avalanche photodiodes with separated absorption and multiplication regions, IEEE J. Quantum Electron. 17 (1981) 243–250, https://doi.org/10.1109/JQE.1981.1071059.
[12] Y.M. El-Batawy, M.J. Deen, Analysis and circuit modeling of waveguide-separated absorption charge multiplication-avalanche photodetector (WG-SACM-APD), IEEE Trans. Electron Devices. 52 (2005) 335–344, https://doi.org/10.1109/TED.2005.843884.
[13] J.C. Yu, L.E. Tarof, T. Baird, D. McGhan, R. Bruce, D.G. Knight, Temperature characterization of separate absorption, grading, charge, and multiplication InP/InGaAs avalanche photodiodes, in: Technol. Opt. Fiber Commun., SPIE, 1994, pp. 302–310. 10.1117/12.175270.
[14] R. Xie, Q. Li, P. Wang, X. Chen, W. Lu, H. Guo, L. Chen, W. Hu, Spatial description theory of narrow-band single-carrier avalanche photodetectors, Opt. Express. 29 (2021) 16432–16446, https://doi.org/10.1364/OE.418110.
[15] W. Hu, X. Chen, F. Yin, Z. Ye, C. Lin, X.N. Hu, Z. Quan, Z. Li, W. Lu, Simulation and design consideration of photoresponse for HgCdTe infrared photodiodes, Opt. Quantum Electron. 40 (2008) 1255–1260, https://doi.org/10.1007/s11082-009-9302-5.
[16] W. Hu, X. Chen, Z. Ye, A. Feng, F. Yin, B. Zhang, L. Liao, W. Lu, Dependence of Ion-Implant-Induced LBIC Novel Characteristic on Excitation Intensity for Long-Wavelength HgCdTe-Based Photovoltaic Infrared Detector Pixel Arrays, IEEE J. Sel. Top. Quantum Electron. 19 (2013) 1–7, https://doi.org/10.1109/JSTQE.2013.2257992.
[17] A. Singh, V. Srivastav, R. Pal, HgCdTe avalanche photodiodes: A review, Opt. Laser Technol. 43 (2011) 1358–1370, https://doi.org/10.1016/j.optlastec.2011.03.009.
[18] S. Velicu, J. Zhao, M. Morley, A.M. Itsuno, J.D. Phillips, Theoretical and experimental investigation of MWIR HgCdTe nBn detectors, in: Quantum Sens. Nanophotonic Devices IX, SPIE, 2012, pp. 635–647, https://doi.org/10.1117/12.904916.
[19] I.N. Yakovkin, N.V. Petrova, Band inversion and absence of surface states in IV – VI semiconductors, Phys. Lett. A. 403 (2021) 127398, https://doi.org/10.1016/j.physleta.2021.127398.
[20] L. Yang, H. Guo, C. Shen, H. Xie, D. Yang, L. Zhu, F. Wang, Q. Sun, L. Chen, C. Lin, L. He, Modeling and characteristics of MWIR HgCdTe APD at different post-annealing processes, Infrared Phys. Technol. 127 (2022) 104413, https://doi.org/10.1016/j.infrared.2022.104413.
[21] W. Qiu, W. Hu, L. Chen, C. Lin, X. Cheng, X. Chen, W. Lu, Dark Current Transport and Avalanche Mechanism in HgCdTe Electron-Avalanche Photodiodes, IEEE Trans. Electron Devices. 62 (2015) 1926–1931, https://doi.org/10.1109/TED.2015.2417193.
[22] P. Martyniuk, Interband Quantum Cascade Infrared Photodetectors: Current Status and Future Trends, Phys. Rev. Appl. 17 (2022) 027001, https://doi.org/10.1103/PhysRevApplied.17.027001.
[23] M.A. Kinch, A Theoretical Model for the HgCdTe Electron Avalanche Photodiode, J. Electron. Mater. 37 (2008) 1453–1459, https://doi.org/10.1007/s11664-008-0439-y.
[24] S. Derelle, S. Bernhardt, R. Hardar, Jé. Primot, J. Deschamps, J. Rothman, A Monte Carlo Study of Hg0.7Cd0.3Te e-APD, IEEE Trans. Electron Dev. 56 (2009) 569–577, https://doi.org/10.1109/TED.2009.2012526.
[25] R.J. McIntyre, A new look at impact ionization-Part I: A theory of gain, noise, breakdown probability, and frequency response, IEEE Trans. Electron Devices. 46 (1999) 1623–1631, https://doi.org/10.1109/16.777150.
[26] G. Perrais, S. Derelle, L. Mollard, J.-P. Chamonal, G. Destefanis, G. Vincent, S. Bernhardt, J. Rothman, Study of the Transit-Time Limitations of the Impulse Response in Mid-Wave Infrared HgCdTe Avalanche Photodiodes, J. Electron. Mater. 38 (2009) 1790–1799, https://doi.org/10.1007/s11664-009-0802-7.
[27] J.W. Harrison, Alloy scattering in ternary III-V compounds, Phys. Rev. B. 13 (1976) 5347–5350, https://doi.org/10.1103/PhysRevB.13.5347.
[28] I. Babushkin, W. Kuehn, C. Köhler, S. Skupin, L. Bergé, K. Reimann, M. Woerner, J. Herrmann, T. Elsaesser, Ultrafast Spatiotemporal Dynamics of Terahertz Generation by Ionizing Two-Color Femtosecond Pulses in Gases, Phys. Rev. Lett. 105 (2010) 053903, https://doi.org/10.1103/PhysRevLett.105.053903.
[29] F. Bertazzi, M. Moresco, M. Penna, M. Goano, E. Bellotti, Full-Band Monte Carlo Simulation of HgCdTe APDs, J. Electron. Mater. 39 (2010) 912–917, https://doi.org/10.1007/s11664-010-1198-0.
[30] M.A. Kinch, J.D. Beck, C.-F. Wan, F. Ma, J. Campbell, HgCdTe electron avalanche photodiodes, J. Electron. Mater. 33 (2004) 630–639, https://doi.org/10.1007/s11664-004-0058-1.
[31] J. Rothman, L. Mollard, S. Goût, L. Bonnefond, J. Wlassow, History-Dependent Impact Ionization Theory Applied to HgCdTe e-APDs, J. Electron. Mater. 40 (2011) 1757–1768, https://doi.org/10.1007/s11664-011-1679-9.
[32] J. Rothman, J. Meilhan, G. Perrais, J.-P. Belle, O. Gravrand, Maximum entropy mobility spectrum analysis of HgCdTe heterostructures, J. Electron. Mater. 35 (2006) 1174–1184, https://doi.org/10.1007/s11664-006-0238-2.
[33] J. Rothman, Physics and Limitations of HgCdTe APDs: A Review, J. Electron. Mater. 47 (2018) 5657–5665, https://doi.org/10.1007/s11664-018-6475-3.
[34] A. Dumas, J. Rothman, F. Gibert, D. Édouart, G. Lasfargues, C. Cénac, F. L. Mounier, J. Pellegrino, J.-P. Zanatta, A. Bardoux, F. Tinto, P. Flamant, Evaluation of a HgCdTe e-APD based detector for 2 μm CO_2 DIAL application, Appl. Opt. 56 (2017) 7577–7585, https://doi.org/10.1364/AO.56.007577.
[35] J. Rothman, G. Perrais, E.D. Borniol, P. Castelein, N. Baier, F. Guellec, M. Tchagaspanian, P. Ballet, L. Mollard, S. Gout, A. Perez, M. Fournier, J.-P. Chamonal, P.M. Tribolet, G. Destefanis, HgCdTe APD- focal plane array development at CEA Leti-Minatec, in: Infrared Technol. Appl. XXXIV, SPIE, 2008: pp. 852–863. 10.1117/12.780447.
[36] J. Rothman, G. Lasfargues, J. Abergel, HgCdTe APDs for free space optical communications, in: UnmannedUnattended Sens. Sens. Netw. XI Adv. Free-Space Opt. Commun. Tech. Appl., SPIE, 2015: pp. 102–114. 10.1117/12.2197171.
[37] J. Rothman, G. Lasfargues, B. Delacourt, A. Dumas, F. Gibert, A. Bardoux, M. Boutillier, HgCdTe APDs for time-resolved space applications, CEAS Space J. 9 (2017) 507–516, https://doi.org/10.1007/s12567-017-0169-1.
[38] Y. Gu, R. Xie, P. Wang, Q. Li, Y. Zou, S. Liu, K. Zhang, Y. Wang, H. Wang, F. Wang, L. Chen, W. Hu, Bandwidth Characteristics of Mid-Wavelength Infrared PIN HgCdTe Avalanche Photodiodes, IEEE J. Quantum Electron. 59 (2023) 1–6, https://doi.org/10.1109/JQE.2023.3237242.
[39] Q. Li, J. He, W. Hu, L. Chen, X. Chen, W. Lu, Influencing Sources for Dark Current Transport and Avalanche Mechanisms in Planar and Mesa HgCdTe p-i-n Electron-Avalanche Photodiodes, IEEE Trans. Electron Devices. 65 (2018) 572–576, https://doi.org/10.1109/TED.2017.2783352.
[40] W. Hu, X. Chen, Z. Ye, W. Lu, A hybrid surface passivation on HgCdTe long wave infrared detector with in-situ CdTe deposition and high-density hydrogen plasma modification, Appl. Phys. Lett. 99 (2011) 091101, https://doi.org/10.1063/1.3633103.
[41] F. Dai, F. Wang, H. Ge, R. Xie, R. Jiang, H. Shi, H. Liu, G. Hu, L. Shen, T. Li, W. Hu, Anomalous Non-equilibrium State Response of Long-Wavelength HgCdTe Infrared Detectors, IEEE Electron Device Lett. (2023) 507–512, https://doi.org/10.1109/LED.2023.3335419.
[42] K. Roy, T. Ahmed, H. Dubey, T.P. Sai, R. Kashid, S. Maliakal, K. Hsieh, S. Shamim, A. Ghosh, Number-Resolved Single-Photon Detection with Ultralow Noise van der Waals Hybrid, Adv. Mater. 30 (2018) 1704412, https://doi.org/10.1002/adma.201704412.
[43] Y. Chen, C. Tan, Z. Wang, J. Miao, X. Ge, T. Zhao, K. Liao, H. Ge, Y. Wang, F. Wang, Y. Zhou, P. Wang, X. Zhou, C. Shan, H. Peng, W. Hu, Momentum-matching and band-alignment van der Waals heterostructures for high-efficiency infrared photodetection, Sci. Adv. 8 (2022) eabq1781, https://doi.org/10.1126/sciadv.abq1781.
[44] J. Beck, C. Wan, M. Kinch, J. Robinson, P. Mitra, R. Scritchfield, F. Ma, J. Campbell, The HgCdTe electron avalanche photodiode, J. Electron. Mater. 35 (2006) 1166–1173, https://doi.org/10.1007/s11664-006-0237-3.
[45] J. Rothman, G. Perrais, G. Destefanis, J. Baylet, P. Castelein, J.-P. Chamonal, High performance characteristics in pin MW HgCdTe e-APDs, in: Infrared Technol. Appl. XXXIII, SPIE, 2007: pp. 475–484. 10.1117/12.723465.
[46] J. Rothman, E.D. Borniol, O. Gravrand, S. Bisotto, L. Mollard, F. Guellec, F. Pistone, S. Courtas, X. Lefoule, HgCdTe APD-focal plane array development at DEFIR, in: Electro-Opt. Infrared Syst. Technol. Appl. VII, SPIE, 2010: pp. 183–190. 10.1117/12.865482.
[47] J. Rothman, L. Mollard, S. Bosson, G. Vojetta, K. Foubert, S. Gatti, G. Bonnouvrier, F. Salveti, A. Kerlain, O. Pacaud, Short-Wave Infrared HgCdTe Avalanche Photodiodes, J. Electron. Mater. 41 (2012) 2928–2936, https://doi.org/10.1007/s11664-012-1970-4.
[48] G. Finger, M. Downing, D. Alvarez, D. Ives, L. Mehrgan, M. Meyer, I. Baker, J. Stegmeier, H.J. Weller, Development of HgCdTe large format MBE arrays and noise-free high speed MOVPE EAPD arrays for ground based NIR astronomy, in: B. Cugny, Z. Sodnik, N. Karafolas (Eds.), Int. Conf. Space Opt. — ICSO 2014, SPIE, Tenerife, Canary Islands, Spain, 2017: p. 210. 10.1117/12.2304270.
[49] X. Sun, J.B. Abshire, J.D. Beck, P. Mitra, K. Reiff, G. Yang, HgCdTe avalanche photodiode detectors for airborne and spaceborne lidar at infrared wavelengths, Opt. Express. 25 (2017) 16589–16602, https://doi.org/10.1364/OE.25.016589.
[50] P. Wang, Y. Wang, L. Ye, M. Wu, R. Xie, X. Wang, X. Chen, Z. Fan, J. Wang, W. Hu, Ferroelectric Localized Field-Enhanced ZnO Nanosheet Ultraviolet Photodetector with High Sensitivity and Low Dark Current, Small 14 (2018) 1800492, https://doi.org/10.1002/smll.201800492.
[51] F. Wu, Q. Li, P. Wang, H. Xia, Z. Wang, Y. Wang, M. Luo, L. Chen, F. Chen, J. Miao, X. Chen, W. Lu, C. Shan, A. Pan, X. Wu, W. Ren, D. Jariwala, W. Hu, High efficiency and fast van der Waals hetero-photodiodes with a unilateral depletion region, Nat. Commun. 10 (2019) 4663, https://doi.org/10.1038/s41467-019-12707-3.
[52] S.S. Sunku, A.S. McLeod, T. Stauber, H. Yoo, D. Halbertal, G. Ni, A. Sternbach, B.-Y. Jiang, T. Taniguchi, K. Watanabe, P. Kim, M.M. Fogler, D.N. Basov, Nano-photocurrent Mapping of Local Electronic Structure in Twisted Bilayer Graphene,

Nano Lett. 20 (2020) 2958–2964, https://doi.org/10.1021/acs.nanolett.9b04637.
[53] J. Yin, H. Wang, H. Peng, Z. Tan, L. Liao, L. Lin, X. Sun, A.L. Koh, Y. Chen, H. Peng, Z. Liu, Selectively enhanced photocurrent generation in twisted bilayer graphene with van Hove singularity, Nat. Commun. 7 (2016) 10699, https://doi.org/10.1038/ncomms10699.
[54] B.B. Zhou, P.C. Jerger, K.-H. Lee, M. Fukami, F. Mujid, J. Park, D.D. Awschalom, Spatiotemporal Mapping of a Photocurrent Vortex in Monolayer MoS2 Using Diamond Quantum Sensors, Phys. Rev. X. 10 (2020) 011003, https://doi.org/10.1103/PhysRevX.10.011003.
[55] J. He, P. Wang, Q. Li, F. Wang, Y. Gu, C. Shen, L. Chen, P. Martyniuk, A. Rogalski, X. Chen, W. Lu, W. Hu, Enhanced Performance of HgCdTe Long-Wavelength Infrared Photodetectors With nBn Design, IEEE Trans. Electron Devices. 67 (2020) 2001–2007, https://doi.org/10.1109/TED.2020.2980887.
[56] J. He, Q. Li, P. Wang, F. Wang, Y. Gu, C. Shen, M. Luo, C. Yu, L. Chen, X. Chen, W. Lu, W. Hu, Design of a bandgap-engineered barrier-blocking HOT HgCdTe long-wavelength infrared avalanche photodiode, Opt. Express. 28 (2020) 33556, https://doi.org/10.1364/OE.408526.
[57] Q. Li, F. Wang, P. Wang, L. Zhang, J. He, L. Chen, P. Martyniuk, A. Rogalski, X. Chen, W. Lu, W. Hu, Enhanced Performance of HgCdTe Midwavelength Infrared Electron Avalanche Photodetectors With Guard Ring Designs, IEEE Trans. Electron Devices. 67 (2020) 542–546, https://doi.org/10.1109/TED.2019.2958105.
[58] R. Xie, P. Wang, F. Wang, X. Chen, W. Lu, W. Hu, Simultaneous control of intensity, phase, and polarization in real time under a weak oscillation theory, Opt. Lett. 46 (2021) 1361–1364, https://doi.org/10.1364/OL.412851.
[59] W. Hu, Z. Ye, L. Liao, H. Chen, L. Chen, R. Ding, L. He, X. Chen, W. Lu, 128 × 128 long-wavelength/mid-wavelength two-color HgCdTe infrared focal plane array detector with ultralow spectral cross talk, Opt. Lett. 39 (2014) 5184–5187, https://doi.org/10.1364/OL.39.005184.
[60] A. Jozwikowska, K. Jozwikowski, J. Antoszewski, C.A. Musca, T. Nguyen, R. H. Sewell, J.M. Dell, L. Faraone, Z. Orman, Generation-recombination effects on dark currents in CdTe-passivated midwave infrared HgCdTe photodiodes, J. Appl. Phys. 98 (2005) 014504, https://doi.org/10.1063/1.1946201.
[61] L. Zhu, Z. Deng, J. Huang, H. Guo, L. Chen, C. Lin, B. Chen, Low frequency noise-dark current correlations in HgCdTe infrared photodetectors, Opt. Express. 28 (2020) 23660–23669, https://doi.org/10.1364/OE.399565.
[62] A. Ferron, J. Rothman, O. Gravrand, Modeling of Dark Current in HgCdTe Infrared Detectors, J. Electron. Mater. 42 (2013) 3303–3308, https://doi.org/10.1007/s11664-013-2733-6.
[63] W. Hu, X. Chen, F. Yin, Z. Quan, Z. Ye, X. Hu, Z. Li, W. Lu, Analysis of temperature dependence of dark current mechanisms for long-wavelength HgCdTe photovoltaic infrared detectors, J. Appl. Phys. 105 (2009) 104502, https://doi.org/10.1063/1.3130163.
[64] Z. Ye, W. Hu, W. Yin, J. Huang, C. Lin, X. Hu, R. Ding, X. Chen, W. Lu, L. He, Low-Roughness Plasma Etching of HgCdTe Masked with Patterned Silicon Dioxide, J. Electron. Mater. 40 (2011) 1642–1646, https://doi.org/10.1007/s11664-011-1633-x.
[65] W. Hu, X. Chen, Z. Ye, J. Zhang, F. Yin, C. Lin, Z. Li, W. Lu, Accurate Simulation of Temperature-Dependent Dark Current in HgCdTe Infrared Detectors Assisted by Analytical Modeling, J. Electron. Mater. 39 (2010) 981–985, https://doi.org/10.1007/s11664-010-1121-8.
[66] O. Gravrand, J. Rothman, C. Cervera, N. Baier, C. Lobre, J.P. Zanatta, O. Boulade, V. Moreau, B. Fieque, HgCdTe Detectors for Space and Science Imaging: General Issues and Latest Achievements, J. Electron. Mater. 45 (2016) 4532–4541, https://doi.org/10.1007/s11664-016-4516-3.
[67] A. Singh, A.K. Shukla, R. Pal, High Performance of Midwave Infrared HgCdTe e-Avalanche Photodiode Detector, IEEE Electron Device Lett. 36 (2015) 360–362, https://doi.org/10.1109/LED.2015.2400571.
[68] A. Singh, R. Pal, Impulse response measurement in the HgCdTe avalanche photodiode, Solid-State Electron. 142 (2018) 41–46, https://doi.org/10.1016/j.sse.2018.02.002.
[69] R. Pal, A. Malik, V. Srivastav, B.L. Sharma, V.R. Balakrishnan, V. Dhar, H.P. Vyas, Engineering Interface Composition for Passivation of HgCdTe Photodiodes, IEEE Trans. Electron Devices. 53 (2006) 2727–2734, https://doi.org/10.1109/TED.2006.883817.
[70] W. Hassis, O. Gravrand, J. Rothman, S. Benahmed, Low-Frequency Noise Characteristics of HgCdTe Infrared Photodiodes Operating at High Temperatures, J. Electron. Mater. 42 (2013) 3288–3296, https://doi.org/10.1007/s11664-013-2728-3.
[71] O. Gravrand, J. Rothman, B. Delacourt, F. Boulard, C. Lobre, P.h. Ballet, J. L. Santailler, C. Cervera, D. Brellier, N. Péré-Laperne, V. Destefanis, A. Kerlain, Shockley–Read–Hall Lifetime Study and Implication in HgCdTe Photodiodes for IR Detection, J. Electron. Mater. 47 (2018) 5680–5690, https://doi.org/10.1007/s11664-018-6557-2.
[72] Y. Wang, L. Song, Y. Chen, W. Huang, Emerging New-Generation Photodetectors Based on Low-Dimensional Halide Perovskites, ACS Photonics 7 (2020) 10–28, https://doi.org/10.1021/acsphotonics.9b01233.
[73] P. Martyniuk, P. Wang, A. Rogalski, Y. Gu, R. Jiang, F. Wang, W. Hu, Infrared avalanche photodiodes from bulk to 2D materials, Light Sci. Appl. 12 (2023) 212, https://doi.org/10.1038/s41377-023-01259-3.
[74] Y. Gong, W. Tang, W. Hou, Z. Zha, C. Hu, Transformation from a Low-Dimensional Framework to a High-Dimensional Architecture Based on Different Metal Ions: Syntheses, Structures, and Photoluminescences, Inorg. Chem. 45 (2006) 4987–4995, https://doi.org/10.1021/ic052095h.
[75] F. Wang, T. Zhang, R. Xie, A. Liu, F. Dai, Y. Chen, T. Xu, H. Wang, Z. Wang, L. Liao, J. Wang, P. Zhou, W. Hu, Next-Generation Photodetectors beyond Van Der Waals Junctions, Adv. Mater. 35 (2023) 2301197, https://doi.org/10.1002/adma.202301197.
[76] T. Hashizume, G. Schweeger, N. Wu, H. Hasegawa, Novel in situ electrochemical technology for formation of oxide- and defect-free Schottky contact to GaAs and related low-dimensional structures, J. Vac. Sci. Technol. B Microelectron. Nanometer Struct. Process. Meas. Phenom. 12 (1994) 2660–2666, https://doi.org/10.1116/1.587227.
[77] A. Gumprich, J. Liedtke, S. Beck, I. Chirca, T. Potočnik, J.A. Alexander-Webber, S. Hofmann, S. Tappertzhofen, Buried graphene heterostructures for electrostatic doping of low-dimensional materials, Nanotechnology 34 (2023) 265203, https://doi.org/10.1088/1361-6528/acbaa2.
[78] Z. Wang, H. Xia, P. Wang, X. Zhou, C. Liu, Q. Zhang, F. Wang, M. Huang, S. Chen, P. Wu, Y. Chen, J. Ye, S. Huang, H. Yan, L. Gu, J. Miao, T. Li, X. Chen, W. Lu, P. Zhou, W. Hu, Controllable Doping in 2D Layered Materials, Adv. Mater. 33 (2021) 2104942, https://doi.org/10.1002/adma.202104942.
[79] P. Wu, L. Ye, L. Tong, P. Wang, Y. Wang, H. Wang, H. Ge, Z. Wang, Y. Gu, K. Zhang, Y. Yu, M. Peng, F. Wang, M. Huang, P. Zhou, W. Hu, Van der Waals two-color infrared photodetector, Light Sci. Appl. 11 (2022) 1–9, https://doi.org/10.1038/s41377-021-00694-4.
[80] H. Wang, J. Guo, J. Miao, W. Luo, Y. Gu, R. Xie, F. Wang, L. Zhang, P. Wang, W. Hu, Emerging Single-Photon Detectors Based on Low-Dimensional Materials, Small 18 (2022) 2103963, https://doi.org/10.1002/smll.202103963.
[81] A.K. Geim, K.S. Novoselov, The rise of graphene, Nat. Mater. 6 (2007) 183–191, https://doi.org/10.1038/nmat1849.
[82] S. Michael, H.C. Schneider, Impact ionization dynamics in small band-gap two-dimensional materials from a coherent phonon mechanism, Phys. Rev. B. 100 (2019) 035431, https://doi.org/10.1103/PhysRevB.100.035431.
[83] F. Rana, Electron-hole generation and recombination rates for Coulomb scattering in graphene, Phys. Rev. B. 76 (2007) 155431, https://doi.org/10.1103/PhysRevB.76.155431.
[84] S. Tani, F. Blanchard, K. Tanaka, Ultrafast Carrier Dynamics in Graphene under a High Electric Field, Phys. Rev. Lett. 109 (2012) 166603, https://doi.org/10.1103/PhysRevLett.109.166603.
[85] I.V. Oladyshkin, S.B. Bodrov, Y.A. Sergeev, A.I. Korytin, M.D. Tokman, A. N. Stepanov, Optical emission of graphene and electron-hole pair production induced by a strong terahertz field, Phys. Rev. B. 96 (2017) 155401, https://doi.org/10.1103/PhysRevB.96.155401.
[86] A.F. Page, F. Ballout, O. Hess, J.M. Hamm, Nonequilibrium plasmons with gain in graphene, Phys. Rev. B. 91 (2015) 075404, https://doi.org/10.1103/PhysRevB.91.075404.
[87] M. Rezaei, S. Bianconi, L.J. Lauhon, H. Mohseni, A New Approach to Designing High-Sensitivity Low-Dimensional Photodetectors, Nano Lett. 21 (2021) 9838–9844, https://doi.org/10.1021/acs.nanolett.1c03665.
[88] A. Gao, J. Lai, Y. Wang, Z. Zhu, J. Zeng, G. Yu, N. Wang, W. Chen, T. Cao, W. Hu, D. Sun, X. Chen, F. Miao, Y. Shi, X. Wang, Observation of ballistic avalanche phenomena in nanoscale vertical InSe/BP heterostructures, Nat. Nanotechnol. 14 (2019) 217–222, https://doi.org/10.1038/s41565-018-0348-z.
[89] C. Yang, C.J. Barrelet, F. Capasso, C.M. Lieber, Single p-Type/Intrinsic/n-Type Silicon Nanowires as Nanoscale Avalanche Photodetectors, Nano Lett. 6 (2006) 2929–2934, https://doi.org/10.1021/nl062314b.
[90] V. Jain, M. Heurlin, E. Barrigon, L. Bosco, A. Nowzari, S. Shroff, V. Boix, M. Karimi, R.J. Jam, A. Berg, L. Samuelson, M.T. Borgström, F. Capasso, H. Pettersson, InP/InAsP Nanowire-Based Spatially Separate Absorption and Multiplication Avalanche Photodetectors, ACS Photonics 4 (2017) 2693–2698, https://doi.org/10.1021/acsphotonics.7b00389.
[91] S. Lei, F. Wen, L. Ge, S. Najmaei, A. George, Y. Gong, W. Gao, Z. Jin, B. Li, J. Lou, J. Kono, R. Vajtai, P. Ajayan, N.J. Halas, An Atomically Layered InSe Avalanche Photodetector, Nano Lett. 15 (2015) 3048–3055, https://doi.org/10.1021/acs.nanolett.5b00016.
[92] C. Liu, J. Guo, L. Yu, Y. Xiang, H. Xiang, J. Li, D. Dai, High-Speed and High-Responsivity Silicon/Black-Phosphorus Hybrid Plasmonic Waveguide Avalanche Photodetector, ACS Photonics 9 (2022) 1764–1774, https://doi.org/10.1021/acsphotonics.2c00244.
[93] L. Liu, X. Cao, X. Liu, Z. Zhang, X. Wang, Y. Xu, Graphene Nanofilms/Silicon Near-Infrared Avalanche Photodetectors, IEEE Trans. Nanotechnol. 21 (2022) 307–310, https://doi.org/10.1109/TNANO.2022.3185108.
[94] Y. Chen, Y. Wang, Z. Wang, Y. Gu, Y. Ye, X. Chai, J. Ye, Y. Chen, R. Xie, Y. Zhou, Z. Hu, Q. Li, L. Zhang, F. Wang, P. Wang, J. Miao, J. Wang, X. Chen, W. Lu, P. Zhou, W. Hu, Unipolar barrier photodetectors based on van der Waals heterostructures, Nat. Electron. 4 (2021) 357–363, https://doi.org/10.1038/s41928-021-00586-w.
[95] P. Wu, L. Ye, L. Tong, P. Wang, Y. Wang, H. Wang, H. Ge, Z. Wang, Y. Gu, K. Zhang, Y. Yu, M. Peng, F. Wang, M. Huang, P. Zhou, W. Hu, Van der Waals two-color infrared photodetector, Light Sci. Appl. 11 (2022) 6, https://doi.org/10.1038/s41377-021-00694-4.
[96] H. Wang, Z. Li, D. Li, P. Chen, L. Pi, X. Zhou, T. Zhai, Van der Waals Integration Based on Two-Dimensional Materials for High-Performance Infrared Photodetectors, Adv. Funct. Mater. 31 (2021) 2103106, https://doi.org/10.1002/adfm.202103106.
[97] J.G.A. Wehner, E.P.G. Smith, W. Radford, C.L. Mears, Crosstalk Modeling of Small-Pitch Two-Color HgCdTe Photodetectors, J. Electron. Mater. 41 (2012) 2925–2927, https://doi.org/10.1007/s11664-012-2057-y.
[98] H. Xia, M. Luo, W. Wang, H. Wang, T. Li, Z. Wang, H. Xu, Y. Chen, Y. Zhou, F. Wang, R. Xie, P. Wang, W. Hu, W. Lu, Pristine PN junction toward atomic layer

devices, Light Sci. Appl. 11 (2022) 170, https://doi.org/10.1038/s41377-022-00814-8.
[99] F. Wang, Z. Liu, T. Zhang, M. Long, X. Wang, R. Xie, H. Ge, H. Wang, J. Hou, Y. Gu, X. Hu, Z. Song, S. Wang, Q. Dong, K. Liao, Y. Tu, T. Han, F. Li, Z. Zhang, X. Hou, S. Wang, L. Li, X. Zhang, D. Zhao, C. Shan, L. Shan, W. Hu, Fully Depleted Self-Aligned Heterosandwiched Van Der Waals Photodetectors, Adv. Mater. 34 (2022) 2203283, https://doi.org/10.1002/adma.202203283.
[100] Z. Song, B. Wei, Q. Wang, W. Wang, Z. Cao, L. Zhang, Q. Mu, T. Han, F. Li, X. Zhu, L. Shan, M. Long, High-performance metal electrode-enhanced double parallel p–n heterojunctions photodetector, J. Appl. Phys. 133 (2023) 124502, https://doi.org/10.1063/5.0141523.
[101] Y. Zeng, F. Meng, S. Fan, P. Wang, C. Kou, M. Sun, H. Hu, R. Cao, S. Wageh, O. A. Al-Hartomy, A. Kalam, B. Du, W. Ding, S. Wei, Z. Guo, Q. Wang, H. Zhang, Fully depleted vdW heterojunction based high performance photovoltaic photodetector, J. Materiomics. 9 (2023) 1039–1047, https://doi.org/10.1016/j.jmat.2023.04.001.
[102] Y. Wang, Y. Gu, A. Cui, Q. Li, T. He, K. Zhang, Z. Wang, Z. Li, Z. Zhang, P. Wu, R. Xie, F. Wang, P. Wang, C. Shan, H. Li, Z. Ye, P. Zhou, W. Hu, Fast Uncooled Mid-Wavelength Infrared Photodetectors with Heterostructures of van der Waals on Epitaxial HgCdTe, Adv. Mater. 34 (2022) 2107772, https://doi.org/10.1002/adma.202107772.
[103] Y. Liang, C. Perumal Veeramalai, G. Lin, X. Su, X. Zhang, S. Feng, Y. Xu, C. Li, A review on III–V compound semiconductor short wave infrared avalanche photodiodes, Nanotechnology 33 (2022) 222003, https://doi.org/10.1088/1361-6528/ac5442.
[104] J. Zhang, M.A. Itzler, H. Zbinden, J.-W. Pan, Advances in InGaAs/InP single-photon detector systems for quantum communication, Light Sci. Appl. 4 (2015) e286–e, https://doi.org/10.1038/lsa.2015.59.
[105] C. Tan, J. Clark, J. David, G. Rees, S. Plimmer, R. Tozer, D. Herbert, D. Robbins, W. Leong, J. Newey, Avalanche noise measurement in thin Si p+-i-n+ diodes, Appl. Phys. Lett. 76 (2000) 3926–3928, https://doi.org/10.1063/1.126823.
[106] L. Xu, E. Wu, X. Gu, Y. Jian, G. Wu, H. Zeng, High-speed InGaAs/InP-based single-photon detector with high efficiency, Appl. Phys. Lett. 94 (2009) 161106, https://doi.org/10.1063/1.3120224.
[107] Y. Ma, Y. Zhang, Y. Gu, X. Chen, L. Zhou, S. Xi, H. Li, Low Operating Voltage and Small Gain Slope of InGaAs APDs With p-Type Multiplication Layer, IEEE Photonics Technol. Lett. 27 (2015) 661–664, https://doi.org/10.1109/LPT.2015.2389819.
[108] M.A. Itzler, X. Jiang, M. Entwistle, K. Slomkowski, A. Tosi, F. Acerbi, F. Zappa, S. Cova, Advances in InGaAsP-based avalanche diode single photon detectors, J. Mod. Opt. 58 (2011) 174–200, https://doi.org/10.1080/09500340.2010.547262.
[109] Y. Alimi, V. Pusino, M.J. Steer, D.R.S. Cumming, InSb Avalanche Photodiodes on GaAs Substrates for Mid-Infrared Detection, IEEE Trans. Electron Devices. 67 (2020) 179–184, https://doi.org/10.1109/TED.2019.2956283.
[110] S.D. March, A.H. Jones, J.C. Campbell, S.R. Bank, Multistep staircase avalanche photodiodes with extremely low noise and deterministic amplification, Nat. Photonics. 15 (2021) 468–474, https://doi.org/10.1038/s41566-021-00814-x.
[111] D. Chen, S.D. March, A.H. Jones, Y. Shen, A.A. Dadey, K. Sun, J.A. McArthur, A. M. Skipper, X. Xue, B. Guo, J. Bai, S.R. Bank, J.C. Campbell, Photon-trapping-enhanced avalanche photodiodes for mid-infrared applications, Nat. Photonics. 17 (2023) 594–600, https://doi.org/10.1038/s41566-023-01208-x.
[112] Y. Liu, S.R. Forrest, J. Hladky, M.J. Lange, G.H. Olsen, D.E. Ackley, A planar InP/InGaAs avalanche photodiode with floating guard ring and double diffused junction, J. Light. Technol. 10 (1992) 182–193, https://doi.org/10.1109/50.120573.
[113] Y. Xiao, M.J. Deen, Temperature dependent studies of InP/InGaAs avalanche photodiodes based on time domain modeling, IEEE Trans. Electron Devices. 48 (2001) 661–670, https://doi.org/10.1109/16.915678.
[114] N. Duan, S. Wang, F. Ma, N. Li, J.C. Campbell, C. Wang, L.A. Coldren, High-speed and low-noise SACM avalanche photodiodes with an impact-ionization-engineered multiplication region, IEEE Photonics Technol. Lett. 17 (2005) 1719–1721, https://doi.org/10.1109/LPT.2005.851903.
[115] A.R. Dixon, J.F. Dynes, Z.L. Yuan, A.W. Sharpe, A.J. Bennett, A.J. Shields, Ultrashort dead time of photon-counting InGaAs avalanche photodiodes, Appl. Phys. Lett. 94 (2009) 231113, https://doi.org/10.1063/1.3151864.
[116] G.M. Williams, M. Compton, D.A. Ramirez, M.M. Hayat, A.S. Huntington, Multi-Gain-Stage InGaAs Avalanche Photodiode With Enhanced Gain and Reduced Excess Noise, IEEE J. Electron Devices Soc. 1 (2013) 54–65, https://doi.org/10.1109/JEDS.2013.2258072.